# NIST SPECIAL PUBLICATION 260-147

U. S. DEPARTMENT OF COMMERCE/Technology Administration National Institute of Standards and Technology

Standard Reference Materials®

Certification of the Rheological Behavior of SRM 2491, Polydimethylsiloxane

Carl R. Schultheisz, Kathleen M. Flynn, and Stefan D. Leigh



**National Institute of Standards and Technology** 

Technology Administration, U.S. Department of Commerce

## **NIST Special Publication 260-147**

Standard Reference Materials®

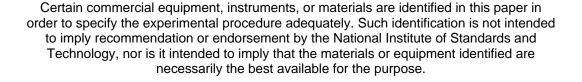
# Certification of the Rheological Behavior of SRM 2491, Polydimethylsiloxane

Carl R. Schultheisz<sup>1</sup>, Kathleen M. Flynn<sup>1</sup>, and Stefan D. Leigh<sup>2</sup>

<sup>1</sup>Polymers Division, Materials Science and Engineering Laboratory <sup>2</sup>Statistical Engineering Division, Information Technology Laboratory National Institute of Standards and Technology Gaithersburg, MD 20899-8541



U.S. DEPARTMENT OF COMMERCE, Donald L. Evans, Secretary
TECHNOLOGY ADMINISTRATION, Phillip J. Bond, Under Secretary of Commerce for Technology
NATIONAL INSTITUTE OF STANDARDS AND TECHNOLOGY, Arden L. Bement, Jr., Director



National Institute of Standards and Technology Special Publication 260-147 Natl. Inst. Stand. Technol. Spec. Publ. 260-147, 88 pages (November 2003) CODEN: NSPUE2

# U.S. GOVERNMENT PRINTING OFFICE WASHINGTON: 2003

#### NIST Special Publication 260-147

### Certification of the Rheological Behavior of SRM 2491, Polydimethylsiloxane

## **Table of Contents**

Abstract	1
1. Introduction	2
2. Preparation, Bottling, and Sampling of SRM 2491	2
3. Testing	4
3.1 Steady Shear Testing for Certification at 25 °C	5
3.2 Steady Shear Testing for Certification at 50 °C	5
3.3 Steady Shear Testing for Certification at 0 °C	6
3.4 Dynamic Testing for Certification	7
4. Analysis of Sources of Uncertainty	9
4.1 Steady Shear Testing in the Cone and Plate Fixtures	9
4.2 Dynamic Testing in Parallel Plates	29
5. Conclusion	61
6. References	71

#### Certification of the Rheological Behavior of SRM 2491, Polydimethylsiloxane

NIST Special Publication 260-147

Carl R. Schultheisz<sup>1</sup>, Kathleen M. Flynn<sup>1</sup> and Stefan D. Leigh<sup>2</sup>

<sup>1</sup>Polymers Division

<sup>2</sup>Statistical Engineering Division

National Institute of Standards and Technology

Gaithersburg, MD 20899

Certain commercial materials and equipment are identified in this paper in order to specify adequately the experimental procedure. In no case does such identification imply recommendation or endorsement by the National Institute of Standards and Technology, nor does it imply necessarily that they are the best available for the purpose.

Final report prepared for the sponsors, the NIST Standard Reference Materials Program (SRMP).

#### **ABSTRACT**

The certification of the rheological properties of Standard Reference Material® (SRM) 2491, a non-Newtonian fluid consisting of polydimethylsiloxane, is described. The viscosity and the first normal stress difference were measured in steady shear at rates between  $0.001~\text{s}^{-1}$  and  $6.3~\text{s}^{-1}$  at 0~°C, 25 °C and 50 °C. The linear viscoelastic storage modulus G' and loss modulus G" were also measured in dynamic oscillatory measurements between 0.1~rad/s and 100~rad/s in the temperature range between 0~°C and 50~°C and master curves calculated using time temperature superposition.

#### 1. Introduction

This report describes the certification of the rheological properties of Standard Reference Material® (SRM) 2491, a non-Newtonian fluid consisting of polydimethylsiloxane. This fluid demonstrates shear thinning (decreasing viscosity with increasing shear rate) and development of normal stresses, which are rheological behaviors common to polymeric materials [1-6]. The viscosity and the first normal stress difference were measured in steady shear at shear rates between  $0.001~\text{s}^{-1}$  and  $6.3~\text{s}^{-1}$  at 0~°C, 25~°C and 50~°C. The linear viscoelastic storage modulus G' and loss modulus G" were also measured in dynamic oscillatory measurements between 0.1~rad/s and 100~rad/s in the temperature range between 0~°C and 50~°C, and master curves were calculated using time temperature superposition.

SRM 2491 is a polymer melt of relatively high molecular mass, and should be free from any problems with stability or evaporation. The polydimethylsiloxane is a commercially available material, and there should be no safety issues.

SRM 2491 accompanies a previous fluid for which NIST has certified the non-Newtonian rheological properties. That fluid is SRM 2490, a solution of polyisobutylene dissolved in 2,6,10,14-tetramethylpentadecane [7]. At 25 °C, the zero-shear-rate viscosity of SRM 2490 is approximately one order of magnitude lower than the zero-shear-rate viscosity of SRM 2491. There were several reasons for investigating a polydimethylsiloxane melt as a Standard Reference Material to accompany the solution used for SRM 2490. First, the polydimethylsiloxane is stable and inert, and therefore should be free from from any problems with chemical stability, evaporation or safety. Secondly, it was expected that the rheological properties of the polydimethylsiloxane melt used for SRM 2491 would have little or no temperature dependence compared to the solution used for SRM 2490. This property could be advantageous in isolating transducer or actuator problems from temperature control problems in a rheometer. However, whereas the temperature dependence of SRM 2491 is less than that of SRM 2490, it is not negligible.

#### 2. Preparation, Bottling, and Sampling of SRM 2491

SRM 2491 consists of polydimethylsiloxane, trimethylsiloxy terminated (Gelest, Inc., catalog number DMS-T61, CAS number 9016-00-6 [8]). The supplier identifies the polydimethylsiloxane as having a number average molecular mass of 308,000 g/mol, with a density of 0.978 g/cm<sup>3</sup> at 25 °C and a volumetric coefficient of thermal expansion of  $9.2 \times 10^{-4}$  cm<sup>3</sup>/(cm<sup>3</sup> K).

The supplier states that the fluid is stable indefinitely at 150 °C in air, and that it has a negligible vapor pressure [8]. Evaporation during testing is therefore not considered a problem, nor is it considered as a source of uncertainty in the measurements.

Homogenization and bottling of SRM 2491 was carried out by Gelest, Inc. Some elevated temperature was used to speed up the bottling process. The solution was packaged in quantities of 100 ml in amber glass bottles, and 273 bottles were delivered to NIST.

The bottles were numbered and filled sequentially. Ten bottles were taken as samples for testing

for certification. One bottle was chosen randomly from each successive sequence of 27 bottles (1-27, 28-54, etc.). This procedure was intended to uncover any systematic variation that might have occurred in the course of the bottling process.

Before each series of tests in the rheometer, the bottles were turned end over end at a rate of one revolution per 10 min for a minimum of 30 min. For turning, the bottles were held with a three-jaw clamp attached to a small motor/gear assembly (McMaster-Carr). Turning the bottles was intended to ensure that the material within each bottle was homogeneous.

#### 3. Testing

All rheological testing was carried out in a Rheometric Scientific, Inc. ARES controlled-strain rheometer. This rheometer employs a force rebalance transducer that measures both torque and normal force. The torque transducer has two ranges, a low range with higher sensitivity for torque with magnitude up to  $0.02~\rm N\cdot m$  ( $200~\rm g_f$  cm, where  $\rm g_f$  indicates a unit of gram force, which is not an acceptable unit of the SI, but is commonly used), and a high range for torque with magnitude up to  $0.2~\rm N\cdot m$  ( $2000~\rm g_f$  cm). The normal force transducer has a single range capable of measuring normal forces up to  $20~\rm N$  ( $2000~\rm g_f$ ) in magnitude. The rheometer transducer was calibrated each day before any testing. Calibration was accomplished following the manufacturer's instructions [9]; the procedure consists of hanging a known mass from a fixture mounted to the transducer to apply a known torque or normal force. The calibration masses were checked on routinely calibrated electronic balances at NIST (OHAUS GA200D for masses of 200 g or less, Mettler PE 3600 for masses greater than 200 g) and found to be within 0.02 % of the specified mass. The dimensions of the calibration fixture were also measured at NIST and found to be within 0.2 % of the specification. For dynamic measurements, the phase angle was also calibrated each day before any testing, again following the manufacturer's instructions.

Four sets of certification tests were conducted. Samples were tested in steady shear at 25 °C, 50 °C and 0 °C (in that order) to determine the viscosity and first normal stress difference as functions of the shear rate. The first set of tests in steady shear at 25 °C was also used to assess the homogeneity of the bottled material, which was used as a criterion for accepting the fluid from the supplier. Subsequently, dynamic tests over a range of frequencies during temperature sweeps from 0 °C to 50 °C were performed to determine the linear viscoelastic properties.

The samples were tested in random order. Typically, two or three samples were tested each day. Steady shear tests were performed by two operators, with one operator doing all of the testing on any given day. The operator sequence was also randomized. All of the dynamic tests were performed by a single operator.

The steady shear tests were performed using cone and plate fixtures, and the dynamic tests were performed using parallel plate fixtures. The fixtures were cleaned with acetone before each experiment. At least once a day, the fixtures were cleaned with toluene and then also cleaned with acetone before use.

Temperature control in the ARES is maintained by a forced air system into an insulated chamber surrounding the test section; the air can be cooled with liquid nitrogen or heated with electrical resistance coils. The mode of temperature control used the platinum resistance thermometer that is in contact with the underside of the lower plate fixture (ARES temperature control mode 2). The temperature control was calibrated before each series of certification tests using a NIST-calibrated thermistor [10] to adjust the parameters in a look-up table. The combined standard uncertainty in the temperature is estimated to be 0.1 °C.

Fresh nitrile or latex gloves were worn for cleaning the fixtures and for loading the samples. Gloves were worn both to prevent skin contact with the material and to prevent contaminating the fixtures or the samples with grease or dirt from the operator's hands. Polydimethylsiloxane is not expected to lead to any health hazards, and no unusual measures were taken for disposing

of the samples after testing.

#### 3.1 Steady Shear Testing for Certification at 25 °C

The fixtures used were 50 mm diameter, 0.0399 rad cone and plate, with the cone truncated at 0.048 mm from its vertex. The tests were run using the Steady Rate Sweep template supplied with the ARES software, taking five points per decade. Tests were performed sweeping from an initial shear rate of 0.001 s<sup>-1</sup> up to a shear rate of 16 s<sup>-1</sup>. The instrument configuration was set to use the Autorange capability of the transducer, but the tests were begun with the torque transducer set to the more sensitive low range. Measurements at each shear rate were made in both the clockwise and counterclockwise directions, with the shear applied for 20 s and then measurements of the torque and normal force averaged over the next 30 s. Before loading each sample, the cone and plate fixtures were installed and set to a nominal gap of 1 mm. The temperature control chamber was then closed and the fixtures brought to 25 °C for 30 min. The gap was then zeroed using the Autozero capability of the ARES (the fixtures brought together until they touched, to establish the baseline from which to set the gap to the proper dimension). The temperature control chamber was then opened, and the upper fixture was raised approximately 60 mm. A sample was then transferred to the lower plate fixture using a 3 mL syringe. The tip end of the syringe was cut off with a utility knife to leave a tube of approximately 1 cm diameter, since the fluid would not easily draw through the normal small diameter tip. The upper cone fixture was lowered to a position of 0.040 mm. The sample was then trimmed flush with the edges of the fixtures, and the cone was repositioned to the specified gap of 0.048 mm. This procedure was used in an effort to compensate for the expansion of the sample and the fixtures when changing from room temperature to the test temperature of 25 °C, in order to achieve the appropriate spherical sample geometry. The temperature control chamber was closed, and the specified Steady Rate Sweep test was started; the test sequence included a 30 min hold at 25 °C to allow the temperature to reach steady state. The total time for a single test was approximately 70 min, including the 30 min delay to ensure thermal steady state before measurements were begun. Two samples were tested from each of the ten bottles, and the twenty samples were tested in a random order. Two or three tests were performed on each day. by one of two operators. The days each operator worked were also chosen randomly.

The normal force measurement is sensitive to the zero position and is strongly affected by temperature fluctuations that cause transient volumetric changes. The zero position of the normal force measurements was adjusted by averaging the first six measurements and subtracting that value from all subsequent measurements. The normal force in that range  $(0.001 \text{ s}^{-1} \text{ to } 0.01 \text{ s}^{-1})$  is well below the sensitivity of the transducer and so can be taken as zero.

#### 3.2 Steady Shear Testing for Certification at 50 °C

The fixtures used were again 50 mm diameter, 0.0399 rad cone and plate, with the cone truncated at 0.048 mm from its vertex. The tests were run using the Steady Rate Sweep template supplied with the ARES software, taking five points per decade. Tests were performed sweeping from an initial shear rate of  $0.001 \text{ s}^{-1}$  up to a shear rate of  $25 \text{ s}^{-1}$ . The instrument configuration was set to use the Autorange capability of the transducer, but the tests were begun with the torque transducer set to the more sensitive low range. Measurements at each shear rate were

made in both the clockwise and counterclockwise directions, with the shear applied for 20 s and then measurements of the torque and normal force averaged over the next 30 s. Before loading each sample, the cone and plate fixtures were installed and set to a nominal gap of 1 mm. The temperature control chamber was then closed and the fixtures brought to 50 °C for 30 min. The gap was then zeroed using the Autozero capability of the ARES (the fixtures brought together until they touched, to establish the baseline from which to set the gap to the proper dimension). The temperature control chamber was then opened, and the upper fixture was raised approximately 60 mm. A sample was then transferred to the lower plate fixture using a 3 mL syringe. The tip end of the syringe was cut off with a utility knife to leave a tube of approximately 1 cm diameter, since the fluid would not easily draw through the normal small diameter tip. The upper cone fixture was lowered to a position of 0.000 mm. The sample was then trimmed flush with the edges of the fixtures, and the cone was repositioned to the specified gap of 0.048 mm. This procedure was used in an effort to compensate for the expansion of the sample and the fixtures when changing from room temperature to the test temperature of 50 °C, in order to achieve the appropriate spherical sample geometry. The temperature control chamber was closed, and the specified Steady Rate Sweep test was started; the test sequence included a 30 min hold at 50 °C to allow the temperature to reach steady state. The total time for a single test was approximately 75 min, including the 30 min delay to ensure thermal steady state before measurements were begun. Two samples were tested from each of the ten bottles, and the twenty samples were tested in a random order. Two or three tests were performed on each day. by one of two operators. The days each operator worked were also chosen randomly.

The normal force measurement is sensitive to the zero position and is strongly affected by temperature fluctuations that cause transient volumetric changes. The zero position of the normal force measurements was adjusted by averaging the first six measurements and subtracting that value from all subsequent measurements. The normal force in that range  $(0.001 \text{ s}^{-1} \text{ to } 0.01 \text{ s}^{-1})$  is well below the sensitivity of the transducer and so can be taken as zero.

#### 3.3 Steady Shear Testing for Certification at 0 °C

The fixtures used were again 50 mm diameter, 0.0399 rad cone and plate, with the cone truncated at 0.048 mm from its vertex. The tests were run using the Steady Rate Sweep template supplied with the ARES software, taking five points per decade. Tests were performed sweeping from an initial shear rate of 0.001 s<sup>-1</sup> up to a shear rate of 16 s<sup>-1</sup>. The instrument configuration was set to use the Autorange capability of the transducer, but the tests were begun with the torque transducer set to the more sensitive low range. Measurements at each shear rate were made in both the clockwise and counterclockwise directions, with the shear applied for 20 s and then measurements of the torque and normal force averaged over the next 30 s. Before loading each sample, the cone and plate fixtures were installed and set to a nominal gap of 1 mm. The temperature control chamber was then closed and the fixtures brought to 0 °C for 30 min. The gap was then zeroed using the Autozero capability of the ARES (the fixtures brought together until they touched, to establish the baseline from which to set the gap to the proper dimension). The temperature control chamber was then opened, and the upper fixture was raised approximately 60 mm. The tool temperature was allowed to reach 15 °C before loading the sample to allow the moisture that condensed on the tool when exposed to the atmosphere to evaporate. A sample was then transferred to the lower plate fixture using a 3 mL syringe. The

tip end of the syringe was cut off with a utility knife to leave a tube of approximately 1 cm diameter, since the fluid would not easily draw through the normal small diameter tip. The upper cone fixture was lowered to a position of 0.096 mm. The sample was then trimmed flush with the edges of the fixtures, and the cone was repositioned to the specified gap of 0.048 mm. This procedure was used in an effort to compensate for the expansion of the sample and the fixtures when changing from room temperature to the test temperature of 0 °C, in order to achieve the appropriate spherical sample geometry. The temperature control chamber was closed, and the specified Steady Rate Sweep test was started; the test sequence included a 30 min hold at 0 °C to allow the temperature to reach steady state. The total time for a single test was approximately 70 min, including the 30 min delay to ensure thermal steady state before measurements were begun. Two samples were tested from each of the ten bottles, and the twenty samples were tested in a random order. Two or three tests were performed on each day, by one of two operators. The days each operator worked were also chosen randomly.

The normal force measurement is sensitive to the zero position and is strongly affected by temperature fluctuations that cause transient volumetric changes. The zero position of the normal force measurements was adjusted by averaging the first six measurements and subtracting that value from all subsequent measurements. The normal force in that range  $(0.001 \text{ s}^{-1} \text{ to } 0.01 \text{ s}^{-1})$  is well below the sensitivity of the transducer and so can be taken as zero.

#### 3.4 Dynamic Testing for Certification

The fixtures used for the dynamic testing were 50 mm diameter parallel plates with a nominal gap of 1 mm. The tests were run using the Dynamic Frequency/Temperature Sweep template supplied with the ARES software. Measurements were taken at 0 °C, 10 °C, 20 °C, 30 °C. 40 °C, and 50 °C; at each temperature the frequency of oscillation increased from 0.1 rad/s to 100 rad/s, taking five points per decade. Tests were performed at a strain magnitude of 2 %, and all data was taken using the more sensitive low range of the torque transducer. The ARES has the capability to adjust the position of the fixtures to compensate for thermal expansion of the test fixtures during the test sequence, so that the gap remains constant throughout the test. The change in the gap caused by thermal expansion of the fixtures was measured to be 1.8 µm/°C (with a standard uncertainty of 0.1 µm/°C). Before loading each sample, the parallel plate fixtures were installed and set to a nominal gap of 1 mm, and then the temperature control chamber was closed and the fixtures brought to 0 °C for 30 min. The gap was then zeroed using the Autozero capability of the ARES (the fixtures brought together until they touched, to establish the baseline from which to calculate the gap). The temperature control chamber was then opened, and the upper fixture was raised approximately 60 mm. The tool temperature was allowed to reach 15 °C before loading the sample to allow the moisture that condensed on the tool when exposed to the atmosphere to evaporate. The sample was centered in the fixtures by turning off the motor and rotating the lower plate while lowering the upper plate. The upper plate was lowered until the sample extruded from the edges of the fixtures at room temperature. The sample was then trimmed flush with the edges of the test fixtures. The temperature control chamber was closed with the temperature setpoint at 0 °C. Cooling to 0 °C required approximately 6 min, after which the temperature control chamber was opened briefly and the upper plate lowered until the sample was flush with the edges of the fixtures at 0 °C. The specified Dynamic Frequency/Temperature Sweep test was started; the test sequence included a

15 min hold at 0 °C to allow the temperature to reach steady state. The subsequent soak time following each 10 °C increment was also set to 15 min. One sample was tested from each of the ten bottles, and the ten samples were tested in a random order. A single operator performed all of the dynamic tests. The total time for each test was approximately 180 min. The minimum gap used was 0.985 mm, and the maximum gap used was 1.100 mm.

#### 4. Analysis of Sources of Uncertainty

Uncertainties from each of the sources that are identified are combined through the mathematical formula for the propagation of uncertainties [11]. For a quantity y that is a function of a number of independent quantities  $x_i$ , with  $y = f(x_i)$ , the combined standard uncertainty in y (symbol  $u_c(y)$ ) is calculated from the standard uncertainty in each  $x_i$  (symbol  $u(x_i)$ ) as

$$u_c^2(y) = \sum_i \left(\frac{\partial f}{\partial x_i}\right)^2 u^2(x_i) \tag{1}$$

For input quantities that are not independent, equation (1) would contain terms involving the covariances, but we will assume that the input variables are independent of one another. An alternative way to express equation (1) is that the combined standard uncertainty in y is the summation in quadrature of the components of the standard uncertainty in y arising from each source  $x_i$ .

$$u_c^2(y) = \sum_i u^2(y, x_i)$$
 (2)

In equation (2),  $u(y, x_i)$  is the component of standard uncertainty in y arising from source  $x_i$ , which includes Type A uncertainties determined through statistical analysis of the data and Type B uncertainties determined from the formula for the propagation of uncertainty and/or determined by any other means [11].

#### 4.1 Steady Shear Testing in the Cone and Plate Fixtures

There are a number of possible sources of uncertainty in the measurements of the viscosity and first normal stress difference. The Type A uncertainties associated with variability in the material and random influences on the test conditions were assessed through multiple measurements.

Those sources of uncertainty considered to be Type B are listed below.

- 1. Temperature
- 2. Transducer
- 3. Rotation rate
- 4. Geometry
  - a. Gap
  - b. Cone angle
  - c. Cone/Plate diameter
  - d. Cone truncation
  - e. Tilt
  - f. Concentricity
- 5. Shear heating
- 6. Inertia-driven secondary flows
- 7. Edge effects
- 8. Surface tension

#### 4.1.1 Uncertainty in the Independent Variables: Temperature and Shear Rate

The viscosity and first normal stress difference are tabulated as functions of temperature and shear rate. The standard uncertainty in the temperature is estimated to be 0.1 °C. The advantage of using the cone and plate is that the shear rate is approximately constant throughout the sample. Uncertainty in the shear rate arises from uncertainties in the rotation rate and in the geometry. The nominal shear rate  $\dot{\gamma}_0$  in the cone and plate is given by

$$\dot{\gamma}_0 = \frac{\omega_0}{\tan \beta_0} \tag{3}$$

where  $\omega_0$  is the specified rate of rotation of the plate, and  $\beta_0$  is the nominal cone angle (0.0399 rad). The standard uncertainty in the rotation rate  $u(\omega)$  is estimated to be  $0.005\omega_0$ , and the standard uncertainty in the cone angle  $u(\beta)$  is estimated to be  $10^{-4}$  rad, based on information from the instrument manufacturer. Measurement of the cone angle at NIST agreed with that given by the manufacturer within that uncertainty. However, it should be noted that Mackay and Dick [12] found much larger uncertainties in a round robin test measuring the geometry of a cone. In equation (3), it is assumed that the cone is perfect and aligned so that the tip would just touch the plate. However, to prevent friction between the fixtures, the tip of the cone is truncated, so there is a small region of decreased shear rate at the center of the fixtures. The manufacturer gives the height of the truncation as 48.3 µm. There is also uncertainty in the gap between the plate and the position of the tip of the cone. The standard uncertainty in the gap is calculated to be 3.5 um. Uncertainty in the gap arises from uncertainties in the cone truncation, uncertainty in position at zero gap and at the specified setting, uncertainty in the flatness of the plate and profile of the cone, compliance of the transducer and thermal expansion of the transducer [9, 13-15]. The standard uncertainty in the cone truncation is taken as 2.5 µm, and the other six influences were each assigned a standard uncertainty of 1 µm. These components of uncertainty were then added in quadrature to calculate the combined standard uncertainty in the gap of 3.5 µm. Tilting of the axis of the cone with respect to the axis of the plate also introduces uncertainty; the standard uncertainty of the angle of tilt is estimated to be  $2 \times 10^{-4}$ rad. The propagation of uncertainties in  $\omega$  and  $\beta$  into the uncertainty in  $\dot{\gamma}$  can be calculated analytically from equation (3). However, uncertainties associated with the cone truncation, the gap and a tilt lead to effects that vary spatially. The uncertainty in the shear rate is therefore calculated through an average over the area of the plate. Incorporating the effects of the truncation, an offset  $h_0$  from the intended gap and an angle of tilt  $\phi$ , the area-averaged shear rate is given by

$$\bar{\gamma} = \frac{1}{\pi R^2} \left[ \int_0^{2\pi} \int_0^{r_1} \frac{\omega r^2}{h_0 + r_1 \tan \beta + \phi \sin \theta} dr d\theta + \int_0^{2\pi} \int_{r_1}^R \frac{\omega r^2}{h_0 + r \tan \beta + \phi \sin \theta} dr d\theta \right]$$
(4)

where  $r_1 = 1.21$  mm is the radius of the truncated region, and R = 25 mm is the outer radius of the cone and plate. Markovitz *et al.* [16] examined the effects of geometry on Newtonian viscosity measurements; the terms describing the tilt in equation (4) follow their analysis. The uncertainty associated with each of these sources was calculated separately, using numerical integration [17]. If the angle of tilt is zero, equation (4) reduces to a one-dimensional integral over r; but for nonzero tilt the integral is fully two-dimensional and was calculated by first integrating over r and then over  $\theta$ . Both the truncation and tilt introduce a bias, which is treated as a standard uncertainty [11]. All of these effects lead to an uncertainty in  $\dot{\gamma}$  that is

proportional to  $\dot{\gamma}$ , and the results are given in Table 1 below. It can be seen that the effects of the tilt are negligible. The combined standard uncertainty is calculated by adding all of the components in quadrature [11].

Table 1. Uncertainty in the Shear Rate							
Source of Uncertainty	Contribution to Standard Uncertainty in <i>γ</i>						
Offset in Gap, $h_0$	0.007×γ						
Rotation Rate, ω	0.005×γ̇						
Cone Angle, $\beta$	0.0025×γ̇						
Cone Truncation	0.001×γ̇						
Angle of Tilt, φ	$2\times10^{-5}\times\dot{\gamma}$						
Combined Standard Uncertainty	0.009×γ̇						

#### 4.1.2 Uncertainties in the Viscosity and First Normal Stress Difference

The Type A uncertainties were assessed through multiple measurements (twenty samples at each temperature using two samples from each of ten randomly chosen bottles) and statistical analysis. Since the intention is to certify the *mean* values of the viscosity and first normal stress difference as functions of shear rate, the Type A uncertainty is calculated by dividing the standard deviation of the twenty measurements by the square root of the number of measurements, yielding the standard uncertainty of the mean. These components of uncertainty are given in Table 3 for the viscosity and Table 4 for the first normal stress difference. Note that the relative Type A uncertainty in the viscosity increases significantly at the highest shear rates for the tests at 0 °C and 25 °C.

The effects of the Type B sources of uncertainty listed above are calculated below. The effects of some of these influences will be calculated using functions fit to the experimental data for the viscosity and first normal stress difference. The viscosity  $\eta(\dot{\gamma}, T)$  has been fit to a Carreau model [4, 6, 18], with

$$\eta(\dot{\gamma},T) = \left(\frac{T\rho}{T_R \rho_R}\right) \eta_R a(T) \left[1 + (\xi_0 a(T)\dot{\gamma})^2\right]^{(n-1)/2}$$
(5)

where  $\dot{\gamma}$  is the shear rate, T is the temperature,  $\rho$  is the density at temperature T,  $\eta_R$  is the zero-shear-rate viscosity at the reference temperature  $T_R = 25$  °C,  $\rho_R$  is the density at the reference temperature  $T_R$  given by the manufacturer as 0.978 g/cm<sup>3</sup> [8],  $\xi_0$  is a parameter that governs the transition from the Newtonian regime at low shear rates to the power law regime at high shear rates, a(T) is the temperature shift factor (discussed below), and n is the power at which the shear stress increases with shear rate. Based on data from the manufacturer [8], n has been set to 0.3. The density is approximated as a linear function of temperature, with  $\rho(T) = \rho_R (1 - \alpha(T - T_R))$ , where  $\alpha$  is the volumetric coefficient of thermal expansion, which is given by the manufacturer

as  $\alpha = 9.2 \times 10^{-4} \text{ cm}^3/(\text{cm}^3 \text{ K})$  [8]. The effect of the change in the density is small compared to the change in the temperature itself.

The temperature dependence is primarily governed by the shift factor a(T), which is equal to the ratio of the zero-shear-rate viscosity at temperature T divided by the zero-shear-rate viscosity at the reference temperature  $T_R = 25$  °C. The shift factor has been fit with a function of the WLF type [6, 18], giving

$$a(T) = \exp\left(\frac{-C_1(T - T_R)}{C_2 + T - T_R}\right)$$
 (6)

The first normal stress difference  $N_1(\dot{\gamma}, T)$  was also fit to an empirical model similar to the Carreau model (using the same temperature shift factor a(T) calculated for the viscosity):

$$N_{1}(\dot{\gamma},T) = \left(\frac{T\rho}{T_{R}\rho_{R}}\right) \psi_{R}(a(T)\dot{\gamma})^{2} \left[1 + (\xi_{1}a(T)\dot{\gamma})^{2}\right]^{(m-1)/2}$$
(7)

In equation (7), T is the temperature,  $\psi_R$  is the zero-shear-rate first normal stress coefficient at the reference temperature  $T_R = 25$  °C,  $\rho$  is the density at temperature  $T_R$ , is the density at the reference temperature  $T_R$ ;  $\xi_1$  and m are parameters fit to the data. Values for the parameters in equations (5) through (7) are given in Table 2.

Table 2. Para	Table 2. Parameters for $\eta(\dot{\gamma}, T)$ , $a(T)$ and $N_1(\dot{\gamma}, T)$									
in the mode	in the models found in equations (5) through (7).									
Parameter	Parameter Value Standard Uncertainty									
$oldsymbol{\eta}_{\scriptscriptstyle R}$	843.9 Pa·s	3.8 Pa·s								
$\xi_0$	0.2037 s	0.0040 s								
n	0.3 [8]									
$C_{I}$	5.20	0.48								
$C_2$	232 °C	21 °C								
$\psi_{\scriptscriptstyle R}$	$200.2 \text{ Pa} \cdot \text{s}^2$	9.6 Pa·s <sup>2</sup>								
$\xi_1$	1.22 s	0.33 s								
m	0.474	0.069								

The measured viscosity  $\eta$  is calculated from the twisting moment M applied to the transducer as

$$\eta = \frac{3\tan\beta_0}{2\pi R_0^3 \omega_0} M \tag{8}$$

where  $R_0 = 25$  mm is the nominal radius of both cone and plate,  $\omega_0$  is the nominal rotation rate and  $\beta_0 = 0.0399$  rad is the nominal cone angle. These nominal values are taken to be constants used in the calculation, with the effects of the uncertainties in R,  $\omega$  and  $\beta$  incorporated through

their effect on the moment M, which is given by the integral over the area of the plate of the radius times the shear stress (the viscosity multiplying the shear rate):

$$M = \int_0^{2\pi} \int_0^R \eta(\dot{\gamma}, T) \dot{\gamma}(r, \theta) r^2 dr d\theta \tag{9}$$

Markovitz *et al.* [16] assessed the effects of geometric imperfections for Newtonian fluids in closed form, and we have adapted their analysis to the non-Newtonian case. This analysis employs the assumption that the shear rate  $\dot{\gamma}$  is given by the relative angular velocity of the plate with respect to the cone divided by the gap between them. If the cone and plate are well aligned (concentric and not tilted), the shear rate at a radius r is approximated as

$$\dot{\gamma} = \frac{\omega r}{h_0 + r \tan \beta} \tag{10}$$

where  $\omega$  is the rate of rotation of the plate,  $h_0$  is an offset spacing between the cone and the plate, and  $\beta$  is the cone angle. Ideally, the offset  $h_0$  would be zero, in which case the shear rate is independent of the radius r. To achieve the condition  $h_0 = 0$  and a constant shear rate throughout most of the sample, the cone is truncated so that the tip of the cone will not touch the plate and cause friction. Approximately 50  $\mu$ m is truncated from the cone, so the radius of the truncated region is approximately 1.25 mm. The truncation allows the cone to lie above or below its intended position, so that  $h_0$  can be either positive or negative. Within the truncated area,  $\beta = 0$ , and the shear rate is a linear function of r, as is the case with parallel plate fixtures. To assess the effects of the cone truncation or nonzero  $h_0$ , equation (9) is evaluated numerically [17], using the viscosity model in equation (5). In general, geometric imperfections affect the moment in the Newtonian case more strongly than in the non-Newtonian case, because with shear thinning, an error that causes an increase in the shear rate is offset somewhat by a decrease in the viscosity.

The uncertainties in the first normal stress difference are addressed in a similar manner, with  $N_1$  determined from the axial force F applied to the transducer.

$$N_1 = \frac{2}{\pi R_0^2} F \tag{11}$$

Again,  $R_0$  is taken to be a constant, and the effects of the uncertainties in each parameter on  $N_1$  are calculated through their effect on F, which is calculated through an integral over the area of the plate similar to that in equation (9). Marsh and Pearson [19] have analyzed the axial force generated in the event that a perfect cone is offset from the plate by an amount  $h_0$ . The force in that case is given by

$$F = \int_0^{2\pi} \int_0^R \frac{(N_1 - N_2)}{2} r dr d\theta + \int_0^{2\pi} \int_0^R \frac{N_2}{2} \left[ \frac{\tan \beta}{h_0 + r \tan \beta} \right] r^2 dr d\theta$$
 (12)

where  $N_2$  is the second normal stress difference. The argument for both  $N_1$  and  $N_2$  in equation (12) is the shear rate  $\dot{\gamma}$  given by equation (10). When  $h_0 = 0$ , equation (12) reduces to the result expected for the cone and plate, in which case the terms containing  $N_2$  cancel:

$$F = \int_0^{2\pi} \int_0^R \frac{N_1}{2} r dr d\theta$$

$$= \frac{\pi R^2 N_1}{2}$$
(13)

For parallel plates, where  $\beta = 0$ , equation (12) reduces to

$$F = \int_0^{2\pi} \int_0^R \frac{(N_1 - N_2)}{2} r dr d\theta \tag{14}$$

To assess the effects of the cone truncation on  $N_1$ , one could assume that equation (14) holds over the truncated area, while the integral in equation (13) holds over the rest of plate (with the radius of the truncated region as the lower limit in the integration instead of 0). To assess the effect of an offset of the cone from the intended position at  $h_0 = 0$ , Marsh and Pearson [19] give an analytical expression for the partial derivative of F with respect to  $h_0$ , evaluated at  $h_0 = 0$ ,

$$\frac{\partial F}{\partial h_0} = \frac{-\pi R}{\tan \beta} \left( \dot{\gamma}_0 \frac{\partial N_1}{\partial \dot{\gamma}_0} + N_2 \right) \tag{15}$$

where  $\dot{\gamma}_0 = \omega/\tan\beta$  is the nominal shear rate. Tanner [3] gives an equivalent expression in a different form. Note that  $N_2$  is typically opposite in sign and smaller in magnitude than  $N_1$ . Since  $N_1$  is a positive, increasing function of  $\dot{\gamma}$ , a conservative estimate of  $\partial F/\partial h_0$  in equation (15) is obtained by taking  $N_2 = 0$ . A conservative estimate of the effect of the cone truncation is also obtained by taking  $N_2 = 0$  in equation (14) applied to the area of the truncation (where the shear rate decreases to zero as the radius approaches zero). Alternatively,  $N_2$  can be calculated from measurements made using parallel plates along with the  $N_1$  data measured with the cone and plate fixtures [1-6].

#### 4.1.2.1 Uncertainty $\eta$ and $N_1$ Arising from Uncertainty in Temperature

The effects of uncertainty in the temperature can be calculated directly from equations (5) through (7) with the parameters in Table 1. For the viscosity, the component of uncertainty associated with uncertainty in the temperature is given by

$$u(\eta, T) = \frac{\partial \eta}{\partial T} u(T)$$

$$= \eta(\dot{\gamma}, T) \left\{ \frac{1}{T} - \frac{\alpha}{1 - \alpha(T - T_R)} + \left[ \frac{1 + n(\xi_0 a(T)\dot{\gamma})^2}{1 + (\xi_0 a(T)\dot{\gamma})^2} \right] \left( \frac{-C_1 C_2}{(C_2 + T - T_R)^2} \right) \right\} u(T)$$
(16)

For the first normal stress difference, the component of uncertainty associated with uncertainty in the temperature is given by

$$u(N_{1},T) = \frac{\partial N_{1}}{\partial T}u(T)$$

$$= N_{1}(\dot{\gamma},T) \left\{ \frac{1}{T} - \frac{\alpha}{1-\alpha(T-T_{R})} + \left[ \frac{2 + (m+1)(\xi_{1}a(T)\dot{\gamma})^{2}}{1 + (\xi_{1}a(T)\dot{\gamma})^{2}} \right] \left( \frac{-C_{1}C_{2}}{(C_{2} + T - T_{R})^{2}} \right) \right\} u(T)$$
(17)

The standard uncertainty in the temperature u(T) is estimated to be 0.1 °C. The components of uncertainty in viscosity and first normal stress difference associated with temperature are given in Tables 3 and 4. Note that these uncertainties represent the effects of temperature on the material properties. Temperature fluctuations also affect the measurement of the normal force directly, because the subsequent thermal expansion and contraction of the sample and the fixtures introduce an axial force on the transducer. These temperature fluctuations are accounted for in the Type A uncertainty calculated from the scatter in the data over repeated tests. The temperature fluctuations in the rheometer are much smaller when heating above the ambient temperature than when cooling below the ambient temperature, because the power to the electric heating system can be varied, whereas the cooling is achieved by the flow of cold air that is

either on or off. There is a larger scatter in the first normal stress difference at 0 °C compared to the scatter at 25 °C or 50 °C, which is particularly noticeable at low levels of  $N_1$ . The scatter in the viscosity data does not show the same dependence on temperature because the thermal fluctuations do not directly affect the measurement of the moment.

#### 4.1.2.2 Uncertainty in $\eta$ and $N_1$ Arising from Uncertainty in Transducer Readings

The effects of uncertainties in the transducer readings can be calculated directly from equations (8) and (11). For the viscosity,

$$u(\eta, M) = \frac{3\tan\beta_0}{2\pi R_0^3 \omega_0} u(M) \tag{18}$$

while for the first normal stress difference,

$$u(N_1, F) = \frac{2}{\pi R_0^2} u(F) \tag{19}$$

The standard uncertainty in the moment is estimated to be  $u(M) = 10^{-7} \text{ N} \cdot \text{m} + 0.002M$ , while the standard uncertainty in the axial force measurement is estimated to be  $u(F) = 8 \times 10^{-4} \text{ N} + 0.002F$ . These estimates are based on information from the instrument manufacturer and the variability observed in the data. The components of uncertainty in viscosity and first normal stress difference associated with the transducer are given in Tables 3 and 4.

#### 4.1.2.3 Uncertainty in $\eta$ and $N_1$ Arising from Uncertainty in Rotation Rate

Uncertainty in the rotation rate affects both the shear rate  $\dot{\gamma}$  and the viscosity in the calculation of the moment M in equation (9). This effect can be calculated using the chain rule to take the derivative of M with respect to  $\dot{\gamma}$  in equation (9), and then take the derivative of  $\dot{\gamma}$  in equation (10) with respect to  $\omega$ , evaluated at  $h_0 = 0$ . Using the model in equation (5) for the viscosity, the component of uncertainty associated with uncertainty in the rotation rate is given by

$$u(\eta,\omega) = \frac{\eta(\dot{\gamma},T)}{\omega_0} \left[ \frac{1 + n(\xi_0 a(T)\dot{\gamma})^2}{1 + (\xi_0 a(T)\dot{\gamma})^2} \right] u(\omega)$$
 (20)

The component of uncertainty in the first normal stress difference associated with uncertainty in the rotation rate can be calculated directyl from the model in equation (7), with

$$u(N_1, \omega) = \frac{N_1(\dot{\gamma}, T)}{\omega_0} \left[ \frac{2 + (m+1)(\xi_1 a(T)\dot{\gamma})^2}{1 + (\xi_1 a(T)\dot{\gamma})^2} \right] u(\omega)$$
 (21)

The standard uncertainty in the rotation rate  $u(\omega)$  is estimated to be  $0.005\omega_0$ , based on information from the instrument manufacturer. The components of uncertainty in viscosity and first normal stress difference associated with rotation rate are given in Tables 3 and 4.

#### 4.1.2.4 Uncertainty in $\eta$ and $N_1$ Arising from Uncertainties Associated with Geometry

#### 4.1.2.4.1 Gap

The effects of uncertainty in the gap were calculated using numerical solution of equations (9) and (12) for the truncated cone geometry with  $h_0 = 1 \mu m$  and  $h_0 = -1 \mu m$  in equation (10). The

partial derivatives of  $\eta$  and  $N_1$  with respect to  $h_0$  were then evaluated at  $h_0 = 0$  for use in equation (1) with the standard uncertainty in the gap estimated to be 3.5 µm. Uncertainty in the gap arises from uncertainties in the cone truncation, uncertainty in position at zero gap and at the specified setting, uncertainty in the flatness of the plate and profile of the cone, compliance of the transducer and thermal expansion of the transducer [9, 13-15]. The standard uncertainty in the cone truncation is taken as 2.5 µm, and the other six influences were each assigned a standard uncertainty of 1 µm. These components of uncertainty were then added in quadrature to calculate the combined standard uncertainty in the gap of 3.5 µm. Equation (15) has been used to estimate the uncertainty in  $N_1$ , with  $N_2 = 0$ . The components of uncertainty in viscosity and first normal stress difference associated with the gap are given in Tables 3 and 4.

#### 4.1.2.4.2 Cone Angle

Effects of uncertainty in the cone angle are evaluated similarly to the effects of uncertainty in the rotation rate. Using the model in equations (5) for the viscosity, the component of uncertainty associated with uncertainty in the cone angle is given by

$$u(\eta, \beta) = \frac{-\eta(\dot{\gamma}, T)}{\cos^2 \beta_0 \tan \beta_0} \left[ \frac{1 + n(\xi_0 a(T)\dot{\gamma})^2}{1 + (\xi_0 a(T)\dot{\gamma})^2} \right] u(\beta)$$
 (22)

Using the model in equation (7) for the first normal stress difference, the component of uncertainty associated with uncertainty in the cone angle is given by

$$u(N_1, \beta) = \frac{-N_1(\dot{\gamma}, T)}{\cos^2 \beta_0 \tan \beta_0} \left[ \frac{2 + (m+1)(\xi_1 a(T)\dot{\gamma})^2}{1 + (\xi_1 a(T)\dot{\gamma})^2} \right] u(\beta)$$
 (23)

Since  $\beta_0 = 0.0399$  rad,  $\cos^2 \beta_0 \approx 1$  and  $\tan \beta_0 \approx \beta_0$ . The standard uncertainty in the cone angle  $u(\beta)$  is estimated to be  $10^{-4}$  rad, based on information from the instrument manufacturer. Measurement of the cone angle at NIST agreed with that given by the manufacturer within that uncertainty. However, it should be noted that Mackay and Dick [12] found much larger uncertainties in a round robin test measuring the geometry of a cone. The components of uncertainty in viscosity and first normal stress difference associated with cone angle are given in Tables 3 and 4.

#### 4.1.2.4.3 Cone/Plate Diameter

For the viscosity, the effects of uncertainties in the diameter of the cone and/or plate are given by

$$u(\eta, R) = \frac{3\eta(\dot{\gamma}, T)}{R_0}u(R) \tag{24}$$

where  $R_0$  is the specified cone/plate diameter, which is 25 mm. For the first normal stress difference, the effects of uncertainties in the diameter of the cone and/or plate are given by

$$u(N_1, R) = \frac{2N_1(\dot{\gamma}, T)}{R_0}u(R)$$
 (25)

The standard uncertainty in the radius of the cone or the plate is estimated to be 0.025 mm. The combined standard uncertainty calculated by adding these two components in quadrature is u(R) = 0.035 mm. The components of uncertainty in viscosity and first normal stress difference associated with cone and/or plate diameter are given in Tables 3 and 4.

#### 4.1.2.4.4 Cone Truncation

The truncation of the cone leads to a region where the shear rate is lower than the nominal shear rate of  $\dot{\gamma}_0 = \omega / \tan \beta$ , which leads to a decrease in the moment and a decrease in the calculated viscosity. The cone truncation therefore introduces a bias. This bias is expressed in the form of a standard uncertainty to be added in quadrature with the other components. For the viscosity, the relative uncertainty associated with the cone truncation is proportional to the cube of the ratio of the diameter of the truncated region to the diameter of the cone/plate; in this case, that ratio is approximately 1/20, so the relative uncertainty in the viscosity is less than  $10^{-4}$ . The component of uncertainty in the viscosity arising from cone truncation has been evaluated numerically using the model in equation (5), and the results are given in Table 3.

For the first normal stress difference, the region of decreased shear rate and the change in the geometry in the truncated region also leads to a bias in the calculated  $N_1$ . In this case, the relative standard uncertainty associated with the cone truncation is proportional to the square of the ratio of the diameter of the truncated region to the diameter of the cone/plate, so the relative standard uncertainty in  $N_1$  is on the order of  $10^{-3}$ . The component of uncertainty in the viscosity arising from cone truncation has been evaluated numerically using the model in equation (7), and the results are given in Table 4.

#### 4.1.2.4.5 Tilt

An angle of tilt between the axis of the cone and the axis of the plate also introduces a bias in the viscosity and first normal stress difference. This angle is expressed as a standard uncertainty estimated to be  $2 \times 10^{-4}$  rad, and the effects of such a tilt were determined by numerical calculation of equations (9) and (13) using the models in equations (5) and (7), along with the expression for the shear rate developed by Markovitz *et al.* [16]. In this case, the shear rate is a function of the angle  $\theta$ , so the integrals in equations (9) and (13) are fully two-dimensional; the numerical evaluation was broken into repeated one-dimensional integrals, first integrating over r and then over  $\theta$ . The components of uncertainty in the viscosity and first normal stress difference arising from a tilt are given in Tables 3 and 4.

#### 4.1.2.4.6 Concentricity

An offset between the axis of the cone and the axis of the plate also introduces a bias in the viscosity and first normal stress difference. This offset is expressed as a standard uncertainty estimated to be 25 µm. The effects of such an offset were also estimated by numerical calculation of equations (9) and (13) using the models in equations (5) and (7). Markovitz *et al.* [16] give an expression for the shear rate as

$$\dot{\gamma}(r,\theta) = \frac{\omega r}{\tan\beta (r^2 + 2br\cos\theta + b^2)^{1/2}}$$
 (26)

where b is the offset between the axis of the cone and the axis of the plate. Again, the integrals in equations (9) and (13) are fully two-dimensional, and the numerical evaluation was broken into repeated one-dimensional integrals, first integrating over r and then over  $\theta$ . In this case, the components of uncertainty in the viscosity and first normal stress difference arising from an offset between the axes of the cone and the plate are negligible compared to other components.

#### 4.1.2.5 Effects of Shear Heating

Energy dissipation through friction can lead to an increase in the temperature in the sample, which would decrease the viscosity and first normal stress difference. Bird, *et al.* [4] suggest that the maximum increase in the temperature caused by shear heating would be

$$\Delta T_{\text{max}} = \frac{\eta \omega^2 R^2}{8k} \tag{27}$$

where k is the thermal conductivity of the fluid. The thermal conductivity of the fluid is given as  $0.16 \text{ W/(m\cdot K)}$  by the manufacturer [8]. The temperature rise associated with shear heating is therefore calculated using equation (27) to be less than  $0.025 \,^{\circ}\text{C}$  over the entire range of conditions reported. Taking this value as a standard uncertainty in the temperature and adding it in quadrature with the standard uncertainty estimated for the temperature control of  $0.1 \,^{\circ}\text{C}$ , the combined standard uncertainty in the temperature is calculated to be  $0.103 \,^{\circ}\text{C}$ . The added effects of shear heating are therefore considered negligible.

#### 4.1.2.6 Inertia-Driven Secondary Flows

The analysis of the cone and plate employs the assumption that the fluid travels in circular paths. Inertial effects can introduce instabilities that alter the assumed flow field and affect the resulting measurements. For the viscosity, these effects are proportional to the square of the Reynolds number Re [6], which is given by

$$Re = \frac{\rho\omega\beta^2 R^2}{\eta_0}$$
 (28)

where  $\rho$  is the fluid density and  $\eta_0$  is the zero-shear-rate viscosity. The relative change in the moment associated with secondary flows is given [6] as

$$\frac{\Delta M}{M} = 6.1 \times 10^{-4} \,\text{Re}^2 \tag{29}$$

Since the Reynolds number is less than  $10^{-6}$  for all the conditions reported, the effect of secondary flow on the moment (and therefore the viscosity measurement) is negligible.

For the first normal stress difference, inertia causes the fluid to try to flow out of the gap between cone and plate, reducing the axial force. The change in the first normal stress difference is given [6] by

$$\Delta N_1 = -0.15 \rho \omega^2 R^2 \tag{30}$$

This bias in the first normal stress difference is treated as a standard uncertainty to be added in quadrature with the other components of uncertainty. This component of uncertainty is given in Table 4. In the calculation, the density has been approximated using the data from the manufacturer [8], using a density of  $0.978 \text{ g/cm}^3$  at 25 °C and a volumetric coefficient of thermal expansion of  $9.2 \times 10^{-4} \text{ cm}^3/(\text{cm}^3 \text{ K})$ .

#### 4.1.2.7 Edge Effects

The conditions at the edge of the cone and plate can impact the measurements in several ways [6], but these effects are not easily quantifiable. Perhaps the most significant difficulty is that the

fluid can escape from between the cone and plate. One indicator of loss of fluid is a decrease in the moment with increasing shear rate. For this fluid, reporting of the data has been limited to those shear rates that could be fit reasonably well with the model in equation (), so the shear rate range has been cut off at rates below where the moment exhibits a decrease with shear rate. Deviation of the experimental data from the model suggests that there could be some alteration in the specimen geometry at the edge, even though the change was insufficient to lead to a decrease in the moment.

#### 4.1.2.8 Surface Tension

Surface tension also affects the measurements [6], particularly the first normal stress difference. These effects have not been quantified, so no component of uncertainty has been assigned to the data.

	Table 3. Components of Standard Uncertainty of the Viscosity										
Temperature	Shear Rate	Measured Viscosity	Standard Uncertainty (Type A)	$u(\eta,T)$	$u(\eta,M)$	$u(\eta,\omega)$	$u(\eta,h_0)$				
°C	s <sup>-1</sup>	Pa⋅s	Pa·s	Pa·s	Pa·s	Pa⋅s	Pa·s				
0.0	0.001000	1472.398	4.917	3.727	6.001	7.362	7.741				
0.0	0.001585	1472.926	5.856	3.728	4.880	7.365	7.743				
0.0	0.002512	1473.684	4.969	3.730	4.165	7.368	7.747				
0.0	0.003981	1476.548	5.311	3.737	3.721	7.383	7.762				
0.0	0.006310	1474.525	5.557	3.732	3.433	7.373	7.752				
0.0	0.01000	1476.258	5.452	3.737	3.258	7.381	7.761				
0.0	0.01585	1476.385	5.353	3.737	3.146	7.382	7.761				
0.0	0.02512	1475.865	5.395	3.735	3.073	7.379	7.758				
0.0	0.03981	1475.193	5.387	3.733	3.027	7.375	7.754				
0.0	0.06310	1475.142	5.347	3.732	2.999	7.373	7.752				
0.0	0.1000	1474.356	5.411	3.728	2.979	7.364	7.743				
0.0	0.1585	1470.268	5.299	3.711	2.960	7.333	7.709				
0.0	0.2512	1465.328	5.298	3.683	2.943	7.280	7.654				
0.0	0.3981	1455.255	5.454	3.619	2.918	7.162	7.530				
0.0	0.6310	1435.874	5.172	3.480	2.877	6.905	7.260				
0.0	1.000	1404.576	4.954	3.205	2.812	6.399	6.728				
0.0	1.585	1356.370	4.854	2.721	2.715	5.513	5.797				
0.0	2.512	1258.286	5.149	2.002	2.518	4.185	4.402				
0.0	3.981	1033.875	4.724	1.200	2.069	2.647	2.784				
0.0	6.310	714.019	5.031	0.611	1.429	1.439	1.514				

Tabl	e 3. (continue	d) Componen	its of Standard	d Uncertainty	of the Viscosity	y
Temperature	Shear Rate	Measured Viscosity	$u(\eta,\beta)$	$u(\eta,R)$	Cone Truncation	Tilt
°C	s <sup>-1</sup>	Pa·s	Pa·s	Pa·s	Pa·s	Pa·s
0.0	0.001000	1472.398	3.694	6.184	0.042	0.019
0.0	0.001585	1472.926	3.695	6.186	0.042	0.018
0.0	0.002512	1473.684	3.697	6.189	0.042	0.019
0.0	0.003981	1476.548	3.705	6.201	0.042	0.019
0.0	0.006310	1474.525	3.699	6.193	0.042	0.019
0.0	0.01000	1476.258	3.704	6.200	0.042	0.019
0.0	0.01585	1476.385	3.704	6.201	0.042	0.019
0.0	0.02512	1475.865	3.703	6.199	0.042	0.019
0.0	0.03981	1475.193	3.701	6.196	0.042	0.018
0.0	0.06310	1475.142	3.700	6.196	0.042	0.019
0.0	0.1000	1474.356	3.695	6.192	0.042	0.019
0.0	0.1585	1470.268	3.679	6.175	0.042	0.018
0.0	0.2512	1465.328	3.653	6.154	0.041	0.018
0.0	0.3981	1455.255	3.594	6.112	0.041	0.018
0.0	0.6310	1435.874	3.465	6.031	0.040	0.016
0.0	1.000	1404.576	3.211	5.899	0.038	0.014
0.0	1.585	1356.370	2.766	5.697	0.034	0.010
0.0	2.512	1258.286	2.100	5.285	0.028	0.006
0.0	3.981	1033.875	1.328	4.342	0.019	0.003
0.0	6.310	714.019	0.722	2.999	0.011	0.002

Та	ble 3. (conti	nued) Com	ponents of Star	ndard Uncert	ainty of the	Viscosity	
Temperature	Shear Rate	Measured Viscosity	Standard Uncertainty (Type A)	$u(\eta,T)$	$u(\eta,M)$	$u(\eta,\omega)$	$u(\eta,h_0)$
°C	s <sup>-1</sup>	Pa·s	Pa·s	Pa·s	Pa·s	Pa·s	Pa·s
25.0	0.001000	841.584	3.433	1.677	4.739	4.208	4.424
25.0	0.001585	842.573	3.689	1.679	3.619	4.213	4.429
25.0	0.002512	844.642	3.343	1.683	2.907	4.223	4.440
25.0	0.003981	843.455	3.717	1.681	2.455	4.217	4.434
25.0	0.006310	844.892	3.244	1.684	2.174	4.224	4.442
25.0	0.01000	844.800	3.293	1.683	1.995	4.224	4.441
25.0	0.01585	844.822	3.301	1.683	1.882	4.224	4.441
25.0	0.02512	844.828	3.282	1.683	1.811	4.224	4.441
25.0	0.03981	844.590	3.322	1.683	1.766	4.223	4.440
25.0	0.06310	844.218	3.308	1.682	1.737	4.221	4.438
25.0	0.1000	844.135	3.291	1.681	1.719	4.219	4.436
25.0	0.1585	843.168	3.334	1.679	1.706	4.213	4.430
25.0	0.2512	841.668	3.317	1.674	1.696	4.201	4.416
25.0	0.3981	839.548	3.346	1.664	1.687	4.179	4.393
25.0	0.6310	833.780	3.358	1.640	1.672	4.121	4.333
25.0	1.000	826.109	3.349	1.595	1.655	4.015	4.222
25.0	1.585	810.034	3.179	1.494	1.622	3.782	3.977
25.0	2.512	785.834	3.394	1.311	1.573	3.358	3.531
25.0	3.981	727.748	3.986	0.998	1.456	2.628	2.764
25.0	6.310	591.084	5.712	0.601	1.183	1.667	1.753

Tab	Table 3. (continued) Components of Standard Uncertainty of the Viscosity										
Temperature	Shear Rate	Measured Viscosity	$u(\eta,\beta)$	$u(\eta,R)$	Cone Truncation	Tilt					
°C	s <sup>-1</sup>	Pa·s	Pa·s	Pa·s	Pa·s	Pa·s					
25.0	0.001000	841.584	2.111	3.535	0.024	0.011					
25.0	0.001585	842.573	2.114	3.539	0.024	0.011					
25.0	0.002512	844.642	2.119	3.547	0.024	0.011					
25.0	0.003981	843.455	2.116	3.543	0.024	0.011					
25.0	0.006310	844.892	2.120	3.549	0.024	0.011					
25.0	0.01000	844.800	2.120	3.548	0.024	0.011					
25.0	0.01585	844.822	2.120	3.548	0.024	0.011					
25.0	0.02512	844.828	2.120	3.548	0.024	0.011					
25.0	0.03981	844.590	2.119	3.547	0.024	0.011					
25.0	0.06310	844.218	2.118	3.546	0.024	0.011					
25.0	0.1000	844.135	2.117	3.545	0.024	0.011					
25.0	0.1585	843.168	2.114	3.541	0.024	0.011					
25.0	0.2512	841.668	2.108	3.535	0.024	0.011					
25.0	0.3981	839.548	2.097	3.526	0.024	0.010					
25.0	0.6310	833.780	2.068	3.502	0.023	0.010					
25.0	1.000	826.109	2.015	3.470	0.023	0.010					
25.0	1.585	810.034	1.898	3.402	0.022	0.009					
25.0	2.512	785.834	1.685	3.301	0.020	0.007					
25.0	3.981	727.748	1.319	3.057	0.017	0.004					
25.0	6.310	591.084	0.836	2.483	0.012	0.002					

Ta	ble 3. (contin	nued) Comp	onents of Stan	dard Uncer	tainty of the	e Viscosity	
Temperature	Shear Rate	Measured Viscosity	Standard Uncertainty (Type A)	$u(\eta,T)$	<i>u</i> (η, <i>M</i> )	$u(\eta,\omega)$	$u(\eta,h_0)$
°C	s <sup>-1</sup>	Pa·s	Pa⋅s	Pa·s	Pa·s	Pa·s	Pa·s
50.0	0.001000	541.393	2.192	0.870	4.139	2.707	2.846
50.0	0.001585	541.337	1.960	0.870	3.017	2.707	2.846
50.0	0.002512	541.815	1.873	0.871	2.301	2.709	2.848
50.0	0.003981	542.264	1.687	0.872	1.852	2.711	2.851
50.0	0.006310	542.137	1.820	0.872	1.569	2.711	2.850
50.0	0.01000	543.487	1.958	0.874	1.393	2.717	2.857
50.0	0.01585	542.361	1.893	0.872	1.278	2.712	2.851
50.0	0.02512	542.906	1.874	0.873	1.207	2.715	2.854
50.0	0.03981	542.492	1.873	0.872	1.162	2.712	2.852
50.0	0.06310	542.664	1.858	0.872	1.134	2.713	2.853
50.0	0.1000	542.159	1.838	0.871	1.115	2.711	2.850
50.0	0.1585	541.768	1.873	0.871	1.103	2.708	2.847
50.0	0.2512	541.398	1.879	0.870	1.095	2.705	2.844
50.0	0.3981	540.468	1.887	0.867	1.089	2.698	2.837
50.0	0.6310	538.982	1.858	0.862	1.083	2.684	2.822
50.0	1.000	535.592	1.861	0.851	1.074	2.650	2.786
50.0	1.585	530.581	1.850	0.828	1.063	2.585	2.718
50.0	2.512	519.971	1.820	0.778	1.041	2.441	2.567
50.0	3.981	499.756	1.699	0.680	1.000	2.161	2.272
50.0	6.310	422.090	1.289	0.476	0.845	1.555	1.636

Tabl	Table 3. (continued) Components of Standard Uncertainty of the Viscosity										
Temperature	Shear Rate	Measured Viscosity	$u(\eta,\beta)$	$u(\eta,R)$	Cone Truncation	Tilt					
°C	s <sup>-1</sup>	Pa·s	Pa·s	Pa·s	Pa·s	Pa·s					
50.0	0.001000	541.393	1.358	2.274	0.015	0.007					
50.0	0.001585	541.337	1.358	2.274	0.015	0.007					
50.0	0.002512	541.815	1.359	2.276	0.015	0.007					
50.0	0.003981	542.264	1.361	2.278	0.015	0.007					
50.0	0.006310	542.137	1.360	2.277	0.015	0.007					
50.0	0.01000	543.487	1.364	2.283	0.015	0.007					
50.0	0.01585	542.361	1.361	2.278	0.015	0.007					
50.0	0.02512	542.906	1.362	2.280	0.015	0.007					
50.0	0.03981	542.492	1.361	2.278	0.015	0.007					
50.0	0.06310	542.664	1.361	2.279	0.015	0.007					
50.0	0.1000	542.159	1.360	2.277	0.015	0.007					
50.0	0.1585	541.768	1.359	2.275	0.015	0.007					
50.0	0.2512	541.398	1.357	2.274	0.015	0.007					
50.0	0.3981	540.468	1.354	2.270	0.015	0.007					
50.0	0.6310	538.982	1.347	2.264	0.015	0.007					
50.0	1.000	535.592	1.330	2.249	0.015	0.007					
50.0	1.585	530.581	1.297	2.228	0.015	0.006					
50.0	2.512	519.971	1.225	2.184	0.014	0.006					
50.0	3.981	499.756	1.084	2.099	0.013	0.004					
50.0	6.310	422.090	0.780	1.773	0.010	0.002					

	Table 4. Components of Uncertainty in the First Normal Stress Difference								
Temper- ature	Shear Rate	Measured $N_1$	Standard Uncertainty (Type A)	$u(N_1,T)$	$u(N_1,F)$	$u(N_1,\boldsymbol{\omega})$	$u(N_1,h_0)$		
°C	s <sup>-1</sup>	Pa	Pa	Pa	Pa	Pa	Pa		
0.0	0.1000	7.255	2.458	0.038	0.829	0.072	0.100		
0.0	0.1585	19.848	2.762	0.103	0.855	0.192	0.270		
0.0	0.2512	39.940	2.211	0.199	0.895	0.374	0.524		
0.0	0.3981	94.788	2.132	0.443	1.004	0.835	1.172		
0.0	0.6310	201.909	2.725	0.877	1.219	1.661	2.331		
0.0	1.000	423.749	2.419	1.738	1.662	3.303	4.634		
0.0	1.585	872.028	5.389	3.459	2.559	6.590	9.244		
0.0	2.512	1783.602	9.790	6.966	4.382	13.283	18.633		
0.0	3.981	3325.021	14.086	12.899	7.465	24.609	34.520		
0.0	6.310	5546.096	29.456	21.456	11.907	40.942	57.431		

Table	Table 4. (continued) Components of Uncertainty in the First Normal Stress Difference									
Temper- ature	Shear Rate	Measured $N_1$	$u(N_1, \boldsymbol{\beta})$	$u(N_1,R)$	Trunc- ation	Tilt	Inertia			
°C	s <sup>-1</sup>	Pa	Pa	Pa	Pa	Pa	Pa			
0.0	0.1000	7.255	0.036	0.020	0.008	$3 \times 10^{-4}$	$1 \times 10^{-6}$			
0.0	0.1585	19.848	0.097	0.056	0.023	$7 \times 10^{-4}$	$4 \times 10^{-6}$			
0.0	0.2512	39.940	0.187	0.112	0.046	0.001	$9 \times 10^{-6}$			
0.0	0.3981	94.788	0.419	0.265	0.106	0.003	$2 \times 10^{-5}$			
0.0	0.6310	201.909	0.834	0.565	0.218	0.005	$6 \times 10^{-5}$			
0.0	1.000	423.749	1.657	1.186	0.443	0.010	$1 \times 10^{-4}$			
0.0	1.585	872.028	3.307	2.442	0.889	0.020	$4 \times 10^{-4}$			
0.0	2.512	1783.602	6.665	4.994	1.794	0.041	$9 \times 10^{-4}$			
0.0	3.981	3325.021	12.348	9.310	3.322	0.076	0.002			
0.0	6.310	5546.096	20.544	15.529	5.524	0.127	0.006			

Tabl	Table 4. (continued) Components of Uncertainty in the First Normal Stress Difference									
Temper- ature	Shear Rate	Measured $N_1$	Standard Uncertainty (Type A)	$u(N_1,T)$	$u(N_1,F)$	$u(N_1,\boldsymbol{\omega})$	$u(N_1,h_0)$			
°C	s <sup>-1</sup>	Pa	Pa	Pa	Pa	Pa	Pa			
25.0	0.1000	2.589	0.400	0.011	0.820	0.026	0.036			
25.0	0.1585	5.398	0.472	0.023	0.826	0.053	0.075			
25.0	0.2512	11.884	0.550	0.049	0.839	0.116	0.163			
25.0	0.3981	29.232	0.489	0.117	0.873	0.278	0.390			
25.0	0.6310	68.024	0.815	0.258	0.951	0.614	0.861			
25.0	1.000	154.542	1.123	0.545	1.124	1.303	1.828			
25.0	1.585	337.510	2.244	1.114	1.490	2.676	3.753			
25.0	2.512	712.182	3.855	2.255	2.239	5.430	7.616			
25.0	3.981	1476.755	7.965	4.578	3.768	11.042	15.489			
25.0	6.310	2755.867	11.334	8.465	6.327	20.430	28.658			

Table 4. (continued) Components of Uncertainty in the First Normal Stress Difference							
Temper- ature	Shear Rate	Measured $N_1$	$u(N_1, \boldsymbol{\beta})$	$u(N_1,R)$	Trunc- ation	Tilt	Inertia
°C	s <sup>-1</sup>	Pa	Pa	Pa	Pa	Pa	Pa
25.0	0.1000	2.589	0.013	0.007	0.003	$1 \times 10^{-4}$	$1 \times 10^{-6}$
25.0	0.1585	5.398	0.027	0.015	0.006	$2 \times 10^{-4}$	$4 \times 10^{-6}$
25.0	0.2512	11.884	0.058	0.033	0.014	$4 \times 10^{-4}$	$9 \times 10^{-6}$
25.0	0.3981	29.232	0.139	0.082	0.034	0.001	$2 \times 10^{-5}$
25.0	0.6310	68.024	0.308	0.190	0.077	0.002	$6 \times 10^{-5}$
25.0	1.000	154.542	0.654	0.433	0.169	0.004	$1 \times 10^{-4}$
25.0	1.585	337.510	1.343	0.945	0.357	0.008	$4 \times 10^{-4}$
25.0	2.512	712.182	2.725	1.994	0.732	0.017	$9 \times 10^{-4}$
25.0	3.981	1476.755	5.541	4.135	1.491	0.034	0.002
25.0	6.310	2755.867	10.251	7.716	2.759	0.064	0.006

Table 4. (continued) Components of Uncertainty in the First Normal Stress Difference							
Temper- ature	Shear Rate	Measured $N_1$	Standard Uncertainty (Type A)	$u(N_1,T)$	$u(N_1,F)$	$u(N_1,\boldsymbol{\omega})$	$u(N_1,h_0)$
°C	s <sup>-1</sup>	Pa	Pa	Pa	Pa	Pa	Pa
50.0	0.3981	8.750	0.427	0.029	0.832	0.086	0.120
50.0	0.6310	23.426	0.431	0.076	0.862	0.223	0.313
50.0	1.000	58.927	0.516	0.182	0.933	0.535	0.750
50.0	1.585	137.343	2.054	0.395	1.090	1.166	1.635
50.0	2.512	308.370	1.961	0.829	1.432	2.457	3.446
50.0	3.981	662.540	3.376	1.704	2.140	5.065	7.105
50.0	6.310	1389.936	16.640	3.494	3.595	10.406	14.597

Table 4. (continued) Components of Uncertainty in the First Normal Stress Difference							
Temper- ature	Shear Rate	Measured $N_1$	$u(N_1, \boldsymbol{\beta})$	$u(N_1,R)$	Trunc- ation	Tilt	Inertia
°C	s <sup>-1</sup>	Pa	Pa	Pa	Pa	Pa	Pa
50.0	0.3981	8.750	0.043	0.024	0.010	$3 \times 10^{-4}$	$2 \times 10^{-5}$
50.0	0.6310	23.426	0.112	0.066	0.027	$8 \times 10^{-4}$	$6 \times 10^{-5}$
50.0	1.000	58.927	0.268	0.165	0.067	0.002	$1 \times 10^{-4}$
50.0	1.585	137.343	0.585	0.385	0.151	0.004	$4 \times 10^{-4}$
50.0	2.512	308.370	1.233	0.863	0.327	0.008	$9 \times 10^{-4}$
50.0	3.981	662.540	2.542	1.855	0.682	0.016	0.002
50.0	6.310	1389.936	5.221	3.892	1.405	0.032	0.006

#### 4.2 Dynamic Testing in Parallel Plates

For the dynamic tests, the uncertainties in the measurements of G' and G" at each temperature and frequency will be estimated. Master curves and the associated shift factors will be calculated using polynomial functions fit to the data in logarithmic space. The curve fitting procedure also provides estimates of the uncertainties in the parameters describing the master curves and shift factors

The Type A uncertainties associated with variability in the material and random influences on the test conditions were assessed through multiple measurements.

Those sources of uncertainty considered to be Type B are listed below.

- 1. Temperature
- 2. Frequency of oscillation
- 3. Cross-correlation procedure
  - a. Transducer reading
  - b. Oscillation magnitude
- 4. Geometry
  - a. Gap
  - b. Plate diameter
  - c. Tilt
  - d. Concentricity
- 5. Inertia
- 6. Edge effects

#### 4.2.1 Uncertainty in the Independent Variables: Temperature and Frequency of Oscillation

The storage modulus G' and loss modulus G" are tabulated as functions of temperature and frequency of oscillation. The standard uncertainty in the temperature is estimated to be 0.1 °C. The standard uncertainty in the frequency of oscillation  $\Omega$  is estimated to be  $10^{-4} \times \Omega$ .

#### 4.2.2 Uncertainties in G' and G"

The Type A uncertainty in each modulus is again calculated from the standard deviation of the repeated experiments divided by the square root of the number of measurements, which gives the uncertainty in the mean of the repeated measurements. These components of uncertainty are listed in Tables 6 and 7.

Type B uncertainties are calculated through the propagation of uncertainties formula in equation (1). These calculations require some analysis of the method by which G' and G" are determined from the geometry, the boundary conditions imposed, and the measured transducer output. The fluid is deformed by oscillating the bottom plate with respect to the upper plate. The strain  $\gamma(t)$  in the fluid can be described as

$$\gamma(t) = \frac{r}{h}\phi(t)$$

$$= \frac{r}{h}\phi_0 \sin(\Omega t + \varepsilon)$$
(31)

where r is the radial position, h is the gap between plates, and  $\phi(t)$  describes the angular position of the lower plate with respect to the upper plate. The function  $\phi(t)$  is assumed to be a sine wave with magnitude of oscillation  $\phi_0$ , frequency of oscillation  $\Omega$ , and a possible phase offset of  $\varepsilon$  between the master driving signal at  $\sin \Omega t$  and the resulting oscillation of the plate. The resulting shear stress  $\tau(t)$  in the fluid is assumed as

$$\tau(t) = G' \frac{r}{h} \phi_0 \sin(\Omega t + \varepsilon) + G'' \frac{r}{h} \phi_0 \cos(\Omega t + \varepsilon)$$

$$= |G^*| \frac{r}{h} \phi_0 \sin(\Omega t + \delta + \varepsilon)$$
(32)

where G' is the storage modulus, G'' is the loss modulus,  $|G^*|$  is the magnitude of the complex modulus and  $\delta$  is the phase offset between the strain and the stress. These parameters are related, with

$$G' = |G^*| \cos \delta$$

$$G'' = |G^*| \sin \delta$$

$$|G^*|^2 = (G')^2 + (G'')^2$$

$$\tan \delta = \frac{G''}{G'}$$
(33)

The moment *M* measured by the transducer is a function of time, and is calculated by integrating over the area of the plate the product of the shear stress and the radial position.

$$M(t) = \int_{0}^{2\pi R} \left[ G' \frac{r^3}{h} \phi_0 \sin(\Omega t + \varepsilon) + G'' \frac{r^3}{h} \phi_0 \cos(\Omega t + \varepsilon) \right] dr d\theta$$

$$= \frac{\pi \phi_0 R^4}{2h} \left[ G' \sin(\Omega t + \varepsilon) + G'' \cos(\Omega t + \varepsilon) \right]$$

$$= \frac{\pi \phi_0 R^4}{2h} \left[ G^* \left| \sin(\Omega t + \delta + \varepsilon) \right| \right]$$

$$= M_0 \sin(\Omega t + \delta + \varepsilon)$$

$$= M_0 \sin(\Omega t + \delta + \varepsilon)$$
(34)

A cross-correlation procedure is used to calculate the storage modulus G' and loss modulus G" from the measured moment M(t) and the measured oscillation  $\phi(t)$  [6, 17, 20, 21]. In principle, this procedure correlates the moment M(t) with the strain to calculate the in-phase storage modulus and with a signal  $\pi/2$  radians out of phase with the strain to calculate the loss modulus. In practice, the cross-correlation procedure is used to calculate the in-phase and out-of-phase components of both the strain and moment compared to master signals. In this procedure, a measured signal is multiplied together with a master signal (either sin  $\Omega t$  or cos  $\Omega t$ ) and the result integrated over one or more periods of oscillation to calculate the magnitude and phase angle of the measured signal with respect to the master signal. This procedure also acts a filter to remove unwanted harmonics and noise [6, 17, 20]. The resulting four calculations are

$$\Phi_{1} = \frac{\Omega}{k\pi} \int_{0}^{2k\pi/\Omega} \phi(t) \sin \Omega t dt = \phi_{0} \cos \varepsilon$$

$$\Phi_{2} = \frac{\Omega}{k\pi} \int_{0}^{2k\pi/\Omega} \phi(t) \cos \Omega t dt = \phi_{0} \sin \varepsilon$$

$$\mathbf{M}_{1} = \frac{\Omega}{k\pi} \int_{0}^{2k\pi/\Omega} M(t) \sin \Omega t dt = \frac{\pi \phi_{0} R^{4}}{2h} [G' \cos \varepsilon - G'' \sin \varepsilon]$$

$$\mathbf{M}_{2} = \frac{\Omega}{k\pi} \int_{0}^{2k\pi/\Omega} M(t) \cos \Omega t dt = \frac{\pi \phi_{0} R^{4}}{2h} [G' \sin \varepsilon + G'' \cos \varepsilon]$$
(35)

where k is the number of cycles over which the integration is performed. The storage and loss moduli are then given by

$$G' = \frac{2h}{\pi R^4} \left[ \frac{\mathbf{M}_1 \Phi_1 + \mathbf{M}_2 \Phi_2}{\Phi_1^2 + \Phi_2^2} \right]$$

$$G'' = \frac{2h}{\pi R^4} \left[ \frac{-\mathbf{M}_1 \Phi_2 + \mathbf{M}_2 \Phi_1}{\Phi_1^2 + \Phi_2^2} \right]$$
(36)

The four quantities  $M_1$ ,  $M_2$ ,  $\Phi_1$  and  $\Phi_2$  are the fundamental outputs from the measurements and the cross-correlation procedure.

The measurements of  $G'(\Omega, T)$  and  $G''(\Omega, T)$  are shifted to create master curves through time-frequency superposition using a shift factor function a(T), with

$$G'(\Omega, T) = \frac{T\rho}{T_R \rho_R} G'(a(T)\Omega, T_R)$$

$$G''(\Omega, T) = \frac{T\rho}{T_R \rho_R} G''(a(T)\Omega, T_R)$$
(37)

where  $T_R = 25$  °C is the reference temperature, and a(T) has the same WLF functional form used in equation (6), giving

$$a(T) = \exp\left(\frac{-C_1(T - T_R)}{C_2 + T - T_R}\right)$$
 (38)

The logarithms of the storage and loss moduli have been fit to polynomial functions of the logarithm of the frequency for calculation of the shift factors [18]. The polynomial functions converge more quickly than an expansion in functions associated with the Rouse modes, and the resulting master curves appear to be satisfactory. The data were fit to functions of the form

$$\ln\left(\frac{G'(\Omega,T)}{1 \text{ Pa}}\right) = \ln\left(\frac{T\rho}{T_R \rho_R}\right) + \sum_{i=0}^{3} p_i \left(\ln\left(\frac{a(T)\Omega}{1 \text{ rad/s}}\right)\right)^i$$

$$\ln\left(\frac{G''(\Omega,T)}{1 \text{ Pa}}\right) = \ln\left(\frac{T\rho}{T_R \rho_R}\right) + \sum_{i=0}^{3} q_i \left(\ln\left(\frac{a(T)\Omega}{1 \text{ rad/s}}\right)\right)^i$$
(39)

Both the storage and loss modulus data were fit simultaneously to the functions in equation (39) to determine the parameters  $C_1$  and  $C_2$  in the temperature shift factor a(T). These functional representations for the storage and loss moduli are also used to calculate the propagation of the

uncertainties in the temperature and in the frequency of oscillation into the uncertainties in the moduli. The calculated parameters are given in Table 5.

Table 5. Parameters for $G'(\Omega, T)$ , $G''(\Omega, T)$ and $a(T)$ in the models found in equations (38) and (39).					
Parameter	Value	Standard Uncertainty			
$p_0$	4.2508	$2.0 \times 10^{-3}$			
$p_1$	1.72838	$8.7 \times 10^{-4}$			
$p_2$	$-9.658 \times 10^{-2}$	$4.6 \times 10^{-4}$			
$p_3$	$-3.09 \times 10^{-3}$	$1.1 \times 10^{-4}$			
$q_0$	6.6701	$1.8 \times 10^{-3}$			
$q_1$	0.95974	$8.6 \times 10^{-4}$			
$q_2$	$-2.790 \times 10^{-2}$	$4.5 \times 10^{-4}$			
$q_3$	$-7.13 \times 10^{-3}$	$1.1 \times 10^{-4}$			
	•	•			
$C_I$	6.64	0.21			
$C_2$	299.4 °C	9.2 °C			

#### 4.2.2.2 Uncertainties Associated with Temperature

The components of the standard uncertainty in G' and G" associated with the standard uncertainty in the temperature can be calculated from the functions in equation (39) using the formula for propagation of uncertainty from equation (1).

$$u(G',T) = \frac{\partial G'}{\partial T}u(T)$$

$$= G'(\Omega,T) \left\{ \frac{1}{T} - \frac{\alpha}{1-\alpha(T-T_R)} + \left( \frac{-C_1C_2}{(C_2+T-T_R)^2} \right) \left[ \sum_{i=1}^3 ip_i \left( \ln\left(\frac{a(T)\Omega}{1 \text{ rad/s}}\right) \right)^{i-1} \right] \right\} u(T)$$

$$u(G'',T) = \frac{\partial G''}{\partial T}u(T)$$

$$= G''(\Omega,T) \left\{ \frac{1}{T} - \frac{\alpha}{1-\alpha(T-T_R)} + \left( \frac{-C_1C_2}{(C_2+T-T_R)^2} \right) \left[ \sum_{i=1}^3 iq_i \left( \ln\left(\frac{a(T)\Omega}{1 \text{ rad/s}}\right) \right)^{i-1} \right] \right\} u(T)$$

The standard uncertainty in the temperature is u(T) = 0.1 °C. The components of the standard uncertainty in G' and G" associated with the standard uncertainty in the temperature are listed in Tables 6 and 7.

## 4.2.2.3 Uncertainties Associated with Frequency of Oscillation

The components of the standard uncertainty in G' and G" associated with the standard uncertainty in the frequency of oscillation  $\Omega$  are also calculated from the functions above fit to the data.

$$u(G',\Omega) = \frac{\partial G'}{\partial \Omega} u(\Omega)$$

$$= \frac{G'(\Omega,T)}{\Omega} \left[ \sum_{i=1}^{3} i p_i \left( \ln \left( \frac{a(T)\Omega}{1 \text{ rad/s}} \right) \right)^{i-1} \right] u(\Omega)$$

$$u(G'',\Omega) = \frac{\partial G''}{\partial \Omega} u(\Omega)$$

$$= \frac{G''(\Omega,T)}{\Omega} \left[ \sum_{i=1}^{3} i q_i \left( \ln \left( \frac{a(T)\Omega}{1 \text{ rad/s}} \right) \right)^{i-1} \right] u(\Omega)$$
(41)

The standard uncertainty in the frequency of oscillation is  $u(\Omega) = 10^{-4} \times \Omega$ . The components of the standard uncertainty in G' and G' associated with the standard uncertainty in the frequency of oscillation are listed in Tables 6 and 7.

# 4.2.2.4 Uncertainties Associated with Cross-correlation of the Transducer Signal and Oscillation Magnitude

The storage modulus G' and loss modulus G" are calculated from cross-correlating the moment and the magnitude of oscillation with master signals of  $\sin \Omega t$  and  $\cos \Omega t$ , as described in connection with equations (35) and (36) above. The cross-correlation procedure does filter out noise and higher harmonics [6, 17, 20]. It seems reasonable to assume that the unwanted signals are no more likely to be correlated with  $\sin \Omega t$  than with  $\cos \Omega t$ , in which case the standard uncertainty in  $\mathbf{M}_1$  should be equal to the standard uncertainty in  $\mathbf{M}_2$ :  $u(\mathbf{M}_1) = u(\mathbf{M}_2)$ . Similarly, the standard uncertainties in  $\Phi_1$  and  $\Phi_2$  should be equal:  $u(\Phi_1) = u(\Phi_2)$ . For this special case, where  $u(\mathbf{M}_1) = u(\mathbf{M}_2)$  and  $u(\Phi_1) = u(\Phi_2)$ , the propagation of the uncertainties into G' and G" have simple forms. Define  $u(\mathbf{M}) \equiv u(\mathbf{M}_1) = u(\mathbf{M}_2)$  and  $u(\Phi) \equiv u(\Phi_1) = u(\Phi_2)$ . The component of standard uncertainty in G' arising from the standard uncertainties in  $\mathbf{M}_1$  and  $\mathbf{M}_2$  is

$$u^{2}(G', \mathbf{M}) \equiv u^{2}(G', \mathbf{M}_{1}, \mathbf{M}_{2}) = \left(\frac{\partial G'}{\partial \mathbf{M}_{1}}\right)^{2} u^{2}(\mathbf{M}_{1}) + \left(\frac{\partial G'}{\partial \mathbf{M}_{2}}\right)^{2} u^{2}(\mathbf{M}_{2})$$

$$= \left(\frac{2h}{\pi R^{4} \phi_{0}}\right)^{2} u^{2}(\mathbf{M})$$
(42)

The component of standard uncertainty in G" arising from the standard uncertainties in  $\mathbf{M}_1$  and  $\mathbf{M}_2$  is the same as that found above for G' (assuming  $u(\mathbf{M}_1) = u(\mathbf{M}_2)$  and  $u(\Phi_1) = u(\Phi_2)$ ):

$$u^{2}(G'', \mathbf{M}) \equiv u^{2}(G'', \mathbf{M}_{1}, \mathbf{M}_{2}) = \left(\frac{2h}{\pi R^{4} \phi_{0}}\right)^{2} u^{2}(\mathbf{M})$$
 (43)

Similarly, the components of standard uncertainty in G' and G" arising from the standard uncertainties in  $\Phi_1$  and  $\Phi_2$  are

$$u^{2}(G', \Phi) \equiv u^{2}(G', \Phi_{1}, \Phi_{2}) = \left(\frac{|G^{*}|}{\phi_{0}}\right)^{2} u^{2}(\Phi)$$

$$u^{2}(G'', \Phi) \equiv u^{2}(G'', \Phi_{1}, \Phi_{2}) = \left(\frac{|G^{*}|}{\phi_{0}}\right)^{2} u^{2}(\Phi)$$
(44)

As mentioned above, the cross-correlation procedure does filter out some extraneous signals. The instrument manufacturer indicates that the constant term in the transducer standard uncertainty is decreased by approximately one order of magnitude, so the standard uncertainty in **M** is taken as  $u(\mathbf{M}) = 10^{-8} \text{ N} \cdot \text{m} + (0.002)M_0$ , where  $M_0$  is the magnitude of the sinusoidally varying moment, as defined by equation (34). The instrument manufacturer also indicates that the standard uncertainty in the magnitude of oscillation is  $u(\Phi) = (0.0025)\phi_0$ . The components of the standard uncertainty in G' and G" associated with the cross correlation procedure are listed in Tables 6 and 7.

#### 4.2.2.5 Uncertainties Associated with Geometry

#### 4.2.2.5.1 Gap

The components of the standard uncertainties in G' and G'' associated with the standard uncertainty in the gap h are given by

$$u(G',h) = \frac{G'}{h_0}u(h)$$

$$u(G'',h) = \frac{G''}{h_0}u(h)$$
(45)

where  $h_0$  is the specified gap. Uncertainty in the gap arises from the uncertainty in the position at zero gap and at the specified setting, uncertainty in the flatness of the upper and lower plates, an angular offset between the planes of the parallel plates, uncertainty in the thermal expansion of the fixtures, compliance of the transducer and thermal expansion of the transducer [9, 13-15]. The deviation from flatness of the parallel plates has a standard uncertainty of 2.5 µm. An angular offset could result in a single point of contact at the edge. This tilting angle has a standard uncertainty of  $2 \times 10^{-4}$  rad, which multiplies the radius of the fixtures to give a standard uncertainty in the position at zero gap of 5 µm. The standard uncertainty in the thermal expansion of the fixtures is 0.1 μm/°C, and the gap was zeroed at 0 °C, so the maximum temperature variation from the known gap dimension is 50 °C. Thus, a value of 5 µm was assigned as a conservative estimate of the standard uncertainty in the gap resulting from uncertainty in the thermal expansion of the fixtures. Each of the other four influences was assigned a standard uncertainty of 1 µm. These components were added in quadrature to calculate a combined standard uncertainty in the gap of  $u(h) = 8.2 \mu m$ . The minimum gap used in the tests was 0.985 mm, so a conservative estimate of  $u(h)/h_0$  is (0.0082/0.985) = 0.0083. The components of the standard uncertainty in G' and G" associated with the standard uncertainty in the gap are listed in Tables 6 and 7.

#### 4.2.2.5.2 Plate Diameter

The components of the standard uncertainties in G' and G" associated with the standard uncertainty in the plate diameter are given by

$$u(G', R) = 4 \frac{G'}{R_0} u(R)$$

$$u(G'', R) = 4 \frac{G''}{R_0} u(R)$$
(46)

where  $R_0 = 25$  mm is the specified plate radius. The standard uncertainty in the radius of the upper or lower plate is estimated to be 0.0025 mm. The combined standard uncertainty calculated by adding these two components in quadrature is u(R) = 0.0035 mm. The components of the standard uncertainty in G' and G" associated with the standard uncertainty in the plate diameter are listed in Tables 6 and 7.

#### 4.2.2.5.3 Tilt

An angle of tilt between the axis of the upper plate and the axis of the lower plate introduces a bias in the measurement of G' and G". This angle is expressed as a standard uncertainty estimated to be  $2 \times 10^{-4}$  rad, and the effects of such a tilt were determined by a two dimensional numerical solution of the integral in equation (34). For a gap of 1 mm, the tilt introduces a component of standard uncertainty in G' of (0.005)G' and a similar component of standard uncertainty in G' of (0.005)G". The components of the standard uncertainty in G' and G" associated with a tilt are listed in Tables 6 and 7.

### 4.2.2.5.4 Concentricity

An offset between the axis of the upper plate and the axis of the lower plate also introduces a bias in the measurement of G' and G''. This offset is expressed as a standard uncertainty estimated to be 25  $\mu$ m. As with the case of measurements in steady shear, the uncertainties in G' and G'' associated with this amount of offset are negligible.

#### 4.2.2.6 Inertia

Inertial effects have been neglected in the equations describing the dynamics of the fluid and the instrument. These influences are not expected to be large, particularly in a strain-controlled rheometer, but the uncertainties associated with inertial effects have not been quantified, so no component of uncertainty has been assigned to the data.

## 4.2.2.7 Edge Effects

In the equations describing the response of the fluid, the geometry is assumed to be a perfect cylinder. The exact shape of the fluid edge will be affected by thermal expansion, surface tension and fluid migration, and the shape of the edge will affect the measurements of G' and G". Again, these effects are not expected to be large, but they have not been quantified, so no component of uncertainty has been assigned to the data.

Table	6. Componen	ts of Standar	d Uncertainty in	n the Storag	ge Modulus	G'
Temperature	Frequency	Storage	Standard	<i>u</i> (G', <i>T</i> )	$u(G',\Omega)$	$u(G',\mathbf{M})$
		Modulus	Uncertainty			
		G'	(Type A)			
°C	rad/s	Pa	Pa	Pa	Pa	Pa
0.0	0.1000	2.950	0.041	0.015	$6 \times 10^{-4}$	0.316
0.0	0.1585	7.275	0.065	0.036	$1 \times 10^{-3}$	0.488
0.0	0.2512	17.712	0.126	0.083	$3 \times 10^{-3}$	0.758
0.0	0.3981	40.890	0.274	0.182	$7 \times 10^{-3}$	1.178
0.0	0.6310	90.429	0.662	0.381	0.015	1.824
0.0	1.000	193.601	1.342	0.769	0.031	2.809
0.0	1.585	395.886	2.802	1.471	0.060	4.279
0.0	2.512	775.449	5.701	2.677	0.109	6.420
0.0	3.981	1448.818	10.253	4.604	0.190	9.459
0.0	6.310	2579.152	17.639	7.462	0.310	13.638
0.0	10.00	4359.395	28.533	11.325	0.474	19.172
0.0	15.85	6978.222	42.775	15.997	0.679	26.208
0.0	25.12	10589.670	59.521	20.930	0.903	34.806
0.0	39.81	15240.340	78.531	25.148	1.112	44.845
0.0	63.10	20890.950	98.540	27.438	1.258	56.154
0.0	100.0	27364.350	119.137	26.443	1.288	68.294

Table 6. (continued) Components of Standard Uncertainty in the Storage Modulus G'								
Temperature	Frequency	Storage Modulus G'	<i>u</i> (G',Φ)	<i>u</i> (G', <i>h</i> )	<i>u</i> (G', <i>R</i> )	Tilt		
°C	rad/s	Pa	Pa	Pa	Pa	Pa		
0.0	0.1000	2.950	0.371	0.024	0.017	0.015		
0.0	0.1585	7.275	0.585	0.060	0.041	0.036		
0.0	0.2512	17.712	0.922	0.147	0.099	0.089		
0.0	0.3981	40.890	1.448	0.339	0.229	0.204		
0.0	0.6310	90.429	2.256	0.751	0.506	0.452		
0.0	1.000	193.601	3.487	1.607	1.084	0.968		
0.0	1.585	395.886	5.324	3.286	2.217	1.979		
0.0	2.512	775.449	8.000	6.436	4.343	3.877		
0.0	3.981	1448.818	11.799	12.025	8.113	7.244		
0.0	6.310	2579.152	17.023	21.407	14.443	12.896		
0.0	10.00	4359.395	23.941	36.183	24.413	21.797		
0.0	15.85	6978.222	32.736	57.919	39.078	34.891		
0.0	25.12	10589.670	43.483	87.894	59.302	52.948		
0.0	39.81	15240.340	56.031	126.495	85.346	76.202		
0.0	63.10	20890.950	70.168	173.395	116.989	104.455		
0.0	100.0	27364.350	85.343	227.124	153.240	136.822		

Table 6. (con	Table 6. (continued) Components of Standard Uncertainty in the Storage Modulus G'									
Temperature	Frequency	Storage Modulus G'	Standard Uncertainty (Type A)	<i>u</i> (G', <i>T</i> )	u(G',Ω)	<i>u</i> (G', <b>M</b> )				
°C	rad/s	Pa	Pa	Pa	Pa	Pa				
10.0	0.1000	1.813	0.054	$9 \times 10^{-3}$	$4 \times 10^{-4}$	0.257				
10.0	0.1585	4.457	0.076	0.021	$9 \times 10^{-4}$	0.395				
10.0	0.2512	11.127	0.125	0.050	$2 \times 10^{-3}$	0.612				
10.0	0.3981	26.400	0.180	0.112	$5 \times 10^{-3}$	0.952				
10.0	0.6310	59.747	0.478	0.241	0.010	1.479				
10.0	1.000	130.639	0.928	0.499	0.022	2.286				
10.0	1.585	275.150	2.124	0.987	0.043	3.506				
10.0	2.512	553.661	4.114	1.852	0.081	5.304				
10.0	3.981	1061.283	7.597	3.285	0.145	7.902				
10.0	6.310	1946.246	14.016	5.519	0.245	11.540				
10.0	10.00	3388.485	23.450	8.696	0.390	16.466				
10.0	15.85	5593.534	36.266	12.794	0.580	22.863				
10.0	25.12	8752.303	53.489	17.491	0.805	30.865				
10.0	39.81	12976.430	73.798	22.060	1.036	40.440				
10.0	63.10	18287.190	94.465	25.455	1.231	51.453				
10.0	100.0	24558.560	115.890	26.380	1.335	63.522				

Table 6. (continued) Components of Standard Uncertainty in the Storage Modulus G'								
Temperature	Frequency	Storage Modulus G'	<i>u</i> (G',Φ)	<i>u</i> (G', <i>h</i> )	<i>u</i> (G', <i>R</i> )	Tilt		
°C	rad/s	Pa	Pa	Pa	Pa	Pa		
10.0	0.1000	1.813	0.296	0.015	0.010	$9 \times 10^{-3}$		
10.0	0.1585	4.457	0.469	0.037	0.025	0.022		
10.0	0.2512	11.127	0.740	0.092	0.062	0.056		
10.0	0.3981	26.400	1.165	0.219	0.148	0.132		
10.0	0.6310	59.747	1.824	0.496	0.335	0.299		
10.0	1.000	130.639	2.833	1.084	0.732	0.653		
10.0	1.585	275.150	4.358	2.284	1.541	1.376		
10.0	2.512	553.661	6.606	4.595	3.101	2.768		
10.0	3.981	1061.283	9.853	8.809	5.943	5.306		
10.0	6.310	1946.246	14.401	16.154	10.899	9.731		
10.0	10.00	3388.485	20.558	28.124	18.976	16.942		
10.0	15.85	5593.534	28.555	46.426	31.324	27.968		
10.0	25.12	8752.303	38.556	72.644	49.013	43.762		
10.0	39.81	12976.430	50.526	107.704	72.668	64.882		
10.0	63.10	18287.190	64.291	151.784	102.408	91.436		
10.0	100.0	24558.560	79.377	203.836	137.528	122.793		

Table 6. (con	ntinued) Com	ponents of St	andard Uncerta	ainty in the	Storage Mo	dulus G'
Temperature	Frequency	Storage	Standard	<i>u</i> (G', <i>T</i> )	$u(G',\Omega)$	$u(G',\mathbf{M})$
		Modulus	Uncertainty			
		G'	(Type A)			
°C	rad/s	Pa	Pa	Pa	Pa	Pa
20.0	0.1000	1.124	0.069	$5 \times 10^{-3}$	$2 \times 10^{-4}$	0.212
20.0	0.1585	2.879	0.065	0.013	$6 \times 10^{-4}$	0.324
20.0	0.2512	7.106	0.068	0.030	$1 \times 10^{-3}$	0.502
20.0	0.3981	17.235	0.229	0.070	$3 \times 10^{-3}$	0.779
20.0	0.6310	40.081	0.370	0.155	$7 \times 10^{-3}$	1.211
20.0	1.000	89.693	0.668	0.329	0.015	1.880
20.0	1.585	193.505	1.518	0.668	0.031	2.898
20.0	2.512	397.996	3.263	1.287	0.060	4.420
20.0	3.981	784.020	5.895	2.357	0.111	6.639
20.0	6.310	1474.124	11.053	4.080	0.194	9.805
20.0	10.00	2636.350	18.659	6.647	0.318	14.159
20.0	15.85	4477.057	29.962	10.142	0.491	19.947
20.0	25.12	7208.341	45.812	14.420	0.707	27.321
20.0	39.81	10985.710	64.793	18.968	0.946	36.344
20.0	63.10	15897.750	87.457	22.952	1.173	46.948
20.0	100.0	21872.700	110.332	25.194	1.336	58.763

Table 6. (continued) Components of Standard Uncertainty in the Storage Modulus G'								
Temperature	Frequency	Storage Modulus G'	<i>u</i> (G',Φ)	<i>u</i> (G', <i>h</i> )	<i>u</i> (G', <i>R</i> )	Tilt		
°C	rad/s	Pa	Pa	Pa	Pa	Pa		
20.0	0.1000	1.124	0.241	$9 \times 10^{-3}$	$6 \times 10^{-3}$	$6 \times 10^{-3}$		
20.0	0.1585	2.879	0.381	0.024	0.016	0.014		
20.0	0.2512	7.106	0.602	0.059	0.040	0.036		
20.0	0.3981	17.235	0.949	0.143	0.097	0.086		
20.0	0.6310	40.081	1.489	0.333	0.224	0.200		
20.0	1.000	89.693	2.325	0.744	0.502	0.448		
20.0	1.585	193.505	3.598	1.606	1.084	0.968		
20.0	2.512	397.996	5.501	3.303	2.229	1.990		
20.0	3.981	784.020	8.274	6.507	4.391	3.920		
20.0	6.310	1474.124	12.231	12.235	8.255	7.371		
20.0	10.00	2636.350	17.674	21.882	14.764	13.182		
20.0	15.85	4477.057	24.909	37.160	25.072	22.385		
20.0	25.12	7208.341	34.126	59.829	40.367	36.042		
20.0	39.81	10985.710	45.406	91.181	61.520	54.929		
20.0	63.10	15897.750	58.661	131.951	89.027	79.489		
20.0	100.0	21872.700	73.429	181.543	122.487	109.364		

Table 6. (con	ntinued) Com	ponents of St	andard Uncerta	ainty in the	Storage Mo	dulus G'
Temperature	Frequency	Storage	Standard	<i>u</i> (G', <i>T</i> )	$u(G',\Omega)$	$u(G',\mathbf{M})$
		Modulus	Uncertainty			
		G'	(Type A)			
°C	rad/s	Pa	Pa	Pa	Pa	Pa
30.0	0.1000	0.704	0.063	$3 \times 10^{-3}$	$2 \times 10^{-4}$	0.178
30.0	0.1585	1.806	0.093	$8 \times 10^{-3}$	$4 \times 10^{-4}$	0.271
30.0	0.2512	4.566	0.099	0.018	$9 \times 10^{-4}$	0.417
30.0	0.3981	11.402	0.107	0.044	$2 \times 10^{-3}$	0.647
30.0	0.6310	27.424	0.251	0.101	$5 \times 10^{-3}$	1.007
30.0	1.000	62.974	0.515	0.221	0.011	1.565
30.0	1.585	138.099	1.027	0.459	0.023	2.421
30.0	2.512	289.962	2.353	0.905	0.045	3.707
30.0	3.981	584.545	4.547	1.702	0.086	5.619
30.0	6.310	1125.264	8.521	3.031	0.154	8.373
30.0	10.00	2065.874	15.149	5.095	0.260	12.232
30.0	15.85	3598.061	25.159	8.028	0.414	17.446
30.0	25.12	5946.615	38.943	11.819	0.617	24.219
30.0	39.81	9300.265	57.676	16.140	0.855	32.672
30.0	63.10	13793.150	79.495	20.344	1.101	42.772
30.0	100.0	19435.980	100.772	23.439	1.307	54.295

Table 6. (continued) Components of Standard Uncertainty in the Storage Modulus G'								
Temperature	Frequency	Storage Modulus G'	<i>u</i> (G',Ф)	<i>u</i> (G', <i>h</i> )	<i>u</i> (G', <i>R</i> )	Tilt		
°C	rad/s	Pa	Pa	Pa	Pa	Pa		
30.0	0.1000	0.704	0.198	$6 \times 10^{-3}$	$4 \times 10^{-3}$	$4 \times 10^{-3}$		
30.0	0.1585	1.806	0.314	0.015	0.010	$9 \times 10^{-3}$		
30.0	0.2512	4.566	0.497	0.038	0.026	0.023		
30.0	0.3981	11.402	0.785	0.095	0.064	0.057		
30.0	0.6310	27.424	1.234	0.228	0.154	0.137		
30.0	1.000	62.974	1.932	0.523	0.353	0.315		
30.0	1.585	138.099	3.002	1.146	0.773	0.690		
30.0	2.512	289.962	4.609	2.407	1.624	1.450		
30.0	3.981	584.545	6.999	4.852	3.273	2.923		
30.0	6.310	1125.264	10.442	9.340	6.301	5.626		
30.0	10.00	2065.874	15.265	17.147	11.569	10.329		
30.0	15.85	3598.061	21.783	29.864	20.149	17.990		
30.0	25.12	5946.615	30.249	49.357	33.301	29.733		
30.0	39.81	9300.265	40.815	77.192	52.081	46.501		
30.0	63.10	13793.150	53.441	114.483	77.242	68.966		
30.0	100.0	19435.980	67.844	161.319	108.841	97.180		

Table 6. (con	Table 6. (continued) Components of Standard Uncertainty in the Storage Modulus G'								
Temperature	Frequency	Storage Modulus G'	Standard Uncertainty (Type A)	<i>u</i> (G', <i>T</i> )	u(G',Ω)	<i>u</i> (G', <b>M</b> )			
°C	rad/s	Pa	Pa	Pa	Pa	Pa			
40.0	0.1000	0.451	0.062	$2 \times 10^{-3}$	$1 \times 10^{-4}$	0.152			
40.0	0.1585	1.239	0.076	$5 \times 10^{-3}$	$3 \times 10^{-4}$	0.229			
40.0	0.2512	3.126	0.102	0.012	$6 \times 10^{-4}$	0.351			
40.0	0.3981	7.772	0.100	0.029	$2 \times 10^{-3}$	0.543			
40.0	0.6310	18.987	0.192	0.067	$4 \times 10^{-3}$	0.844			
40.0	1.000	44.722	0.512	0.151	$8 \times 10^{-3}$	1.314			
40.0	1.585	100.166	0.817	0.320	0.017	2.038			
40.0	2.512	213.897	1.652	0.644	0.034	3.139			
40.0	3.981	439.351	3.337	1.237	0.066	4.781			
40.0	6.310	863.639	6.861	2.258	0.122	7.176			
40.0	10.00	1621.117	12.389	3.900	0.212	10.583			
40.0	15.85	2891.034	21.304	6.327	0.347	15.262			
40.0	25.12	4896.067	34.287	9.614	0.533	21.450			
40.0	39.81	7845.696	51.740	13.581	0.763	29.309			
40.0	63.10	11915.750	72.863	17.758	1.017	38.870			
40.0	100.0	17188.690	97.237	21.344	1.254	50.015			

Table 6. (con	tinued) Comp	onents of Sta	ndard Uncer	tainty in the	Storage Mo	dulus G'
Temperature	Frequency	Storage Modulus G'	<i>u</i> (G',Φ)	<i>u</i> (G', <i>h</i> )	<i>u</i> (G', <i>R</i> )	Tilt
°C	rad/s	Pa	Pa	Pa	Pa	Pa
40.0	0.1000	0.451	0.165	$4 \times 10^{-3}$	$3 \times 10^{-3}$	$2 \times 10^{-3}$
40.0	0.1585	1.239	0.261	0.010	$7 \times 10^{-3}$	$6 \times 10^{-3}$
40.0	0.2512	3.126	0.414	0.026	0.018	0.016
40.0	0.3981	7.772	0.654	0.065	0.044	0.039
40.0	0.6310	18.987	1.030	0.158	0.106	0.095
40.0	1.000	44.722	1.617	0.371	0.250	0.224
40.0	1.585	100.166	2.523	0.831	0.561	0.501
40.0	2.512	213.897	3.899	1.775	1.198	1.069
40.0	3.981	439.351	5.952	3.647	2.460	2.197
40.0	6.310	863.639	8.946	7.168	4.836	4.318
40.0	10.00	1621.117	13.204	13.455	9.078	8.106
40.0	15.85	2891.034	19.053	23.996	16.190	14.455
40.0	25.12	4896.067	26.788	40.637	27.418	24.480
40.0	39.81	7845.696	36.611	65.119	43.936	39.228
40.0	63.10	11915.750	48.563	98.901	66.728	59.579
40.0	100.0	17188.690	62.493	142.666	96.257	85.943

Table 6. (con	ntinued) Com	ponents of St	andard Uncerta	ainty in the	Storage Mo	dulus G'
Temperature	Frequency	Storage	Standard	<i>u</i> (G', <i>T</i> )	$u(G',\Omega)$	$u(G',\mathbf{M})$
		Modulus	Uncertainty			
		G'	(Type A)			
°C	rad/s	Pa	Pa	Pa	Pa	Pa
50.0	0.1000	0.301	0.063	$1 \times 10^{-3}$	$7 \times 10^{-5}$	0.131
50.0	0.1585	0.878	0.074	$3 \times 10^{-3}$	$2 \times 10^{-4}$	0.196
50.0	0.2512	2.103	0.089	$8 \times 10^{-3}$	$4 \times 10^{-4}$	0.298
50.0	0.3981	5.521	0.094	0.020	$1 \times 10^{-3}$	0.459
50.0	0.6310	13.536	0.181	0.046	$3 \times 10^{-3}$	0.713
50.0	1.000	32.173	0.250	0.104	$6 \times 10^{-3}$	1.111
50.0	1.585	72.720	0.609	0.223	0.013	1.726
50.0	2.512	159.061	1.219	0.461	0.026	2.667
50.0	3.981	332.501	2.550	0.904	0.052	4.084
50.0	6.310	665.395	5.451	1.686	0.097	6.170
50.0	10.00	1274.141	9.973	2.982	0.172	9.176
50.0	15.85	2323.171	17.880	4.971	0.290	13.358
50.0	25.12	4025.386	29.611	7.776	0.457	18.988
50.0	39.81	6602.065	45.943	11.332	0.675	26.249
50.0	63.10	10259.591	66.388	15.322	0.928	35.253
50.0	100.0	15120.080	90.879	19.099	1.183	45.896

Table 6. (con	Table 6. (continued) Components of Standard Uncertainty in the Storage Modulus G'								
Temperature	Frequency	Storage Modulus G'	<i>u</i> (G',Φ)	<i>u</i> (G', <i>h</i> )	<i>u</i> (G', <i>R</i> )	Tilt			
°C	rad/s	Pa	Pa	Pa	Pa	Pa			
50.0	0.1000	0.301	0.139	$2 \times 10^{-3}$	$2 \times 10^{-3}$	$2 \times 10^{-3}$			
50.0	0.1585	0.878	0.220	$7 \times 10^{-3}$	$5 \times 10^{-3}$	$4 \times 10^{-3}$			
50.0	0.2512	2.103	0.347	0.017	0.012	0.011			
50.0	0.3981	5.521	0.549	0.046	0.031	0.028			
50.0	0.6310	13.536	0.866	0.112	0.076	0.068			
50.0	1.000	32.173	1.363	0.267	0.180	0.161			
50.0	1.585	72.720	2.133	0.604	0.407	0.364			
50.0	2.512	159.061	3.309	1.320	0.891	0.795			
50.0	3.981	332.501	5.081	2.760	1.862	1.663			
50.0	6.310	665.395	7.687	5.523	3.726	3.327			
50.0	10.00	1274.141	11.445	10.575	7.135	6.371			
50.0	15.85	2323.171	16.673	19.282	13.010	11.616			
50.0	25.12	4025.386	23.710	33.411	22.542	20.127			
50.0	39.81	6602.065	32.786	54.797	36.972	33.010			
50.0	63.10	10259.591	44.041	85.155	57.454	51.298			
50.0	100.0	15120.080	57.345	125.497	84.672	75.600			

Table	e 7. Compone	ents of Standa	rd Uncertainty	in the Loss	Modulus G	,"
Temperature	Frequency	Loss	Standard	<i>u</i> (G", <i>T</i> )	u(G",Ω)	$u(G'',\mathbf{M})$
		Modulus	Uncertainty			
		G"	(Type A)			
°C	rad/s	Pa	Pa	Pa	Pa	Pa
0.0	0.1000	148.182	0.841	0.348	0.015	0.316
0.0	0.1585	233.995	1.362	0.551	0.023	0.488
0.0	0.2512	368.530	2.101	0.862	0.036	0.758
0.0	0.3981	577.815	3.333	1.328	0.056	1.178
0.0	0.6310	897.811	5.189	2.007	0.085	1.824
0.0	1.000	1381.229	7.931	2.967	0.127	2.809
0.0	1.585	2092.364	11.621	4.262	0.183	4.279
0.0	2.512	3104.602	16.728	5.904	0.256	6.420
0.0	3.981	4491.832	24.166	7.827	0.343	9.459
0.0	6.310	6301.695	31.625	9.827	0.438	13.638
0.0	10.00	8526.568	39.495	11.531	0.526	19.172
0.0	15.85	11079.910	48.655	12.424	0.586	26.208
0.0	25.12	13797.660	55.467	11.953	0.597	34.806
0.0	39.81	16433.310	58.199	9.653	0.537	44.845
0.0	63.10	18743.830	63.624	5.334	0.398	56.154
0.0	100.0	20409.260	67.681	0.863	0.181	68.294

Table 7. (continued) Components of Standard Uncertainty in the Loss Modulus G"									
Temperature	Frequency	Loss Modulus G"	<i>u</i> (G",Φ)	<i>u</i> (G", <i>h</i> )	<i>u</i> (G", <i>R</i> )	Tilt			
°C	rad/s	Pa	Pa	Pa	Pa	Pa			
0.0	0.1000	148.182	0.371	1.230	0.830	0.741			
0.0	0.1585	233.995	0.585	1.942	1.310	1.170			
0.0	0.2512	368.530	0.922	3.059	2.064	1.843			
0.0	0.3981	577.815	1.448	4.796	3.236	2.889			
0.0	0.6310	897.811	2.256	7.452	5.028	4.489			
0.0	1.000	1381.229	3.487	11.464	7.735	6.906			
0.0	1.585	2092.364	5.324	17.367	11.717	10.462			
0.0	2.512	3104.602	8.000	25.768	17.386	15.523			
0.0	3.981	4491.832	11.799	37.282	25.154	22.459			
0.0	6.310	6301.695	17.023	52.304	35.289	31.508			
0.0	10.00	8526.568	23.941	70.771	47.749	42.633			
0.0	15.85	11079.910	32.736	91.963	62.047	55.400			
0.0	25.12	13797.660	43.483	114.521	77.267	68.988			
0.0	39.81	16433.310	56.031	136.396	92.027	82.167			
0.0	63.10	18743.830	70.168	155.574	104.965	93.719			
0.0	100.0	20409.260	85.343	169.397	114.292	102.046			

Table 7. (continued) Components of Standard Uncertainty in the Loss Modulus G"									
Temperature	Frequency	Loss	Standard	<i>u</i> (G", <i>T</i> )	u(G",Ω)	$u(G'',\mathbf{M})$			
		Modulus	Uncertainty						
		G"	(Type A)						
°C	rad/s	Pa	Pa	Pa	Pa	Pa			
10.0	0.1000	118.479	0.731	0.256	0.012	0.257			
10.0	0.1585	187.541	1.135	0.410	0.019	0.395			
10.0	0.2512	295.930	1.799	0.646	0.029	0.612			
10.0	0.3981	465.325	2.813	1.004	0.046	0.952			
10.0	0.6310	727.025	4.379	1.535	0.070	1.479			
10.0	1.000	1125.524	6.796	2.299	0.106	2.286			
10.0	1.585	1721.208	10.290	3.358	0.155	3.506			
10.0	2.512	2583.663	14.673	4.747	0.221	5.304			
10.0	3.981	3795.438	21.272	6.458	0.303	7.902			
10.0	6.310	5421.453	29.248	8.368	0.398	11.540			
10.0	10.00	7492.469	37.958	10.212	0.495	16.466			
10.0	15.85	9958.459	47.423	11.554	0.576	22.863			
10.0	25.12	12698.490	55.678	11.876	0.619	30.865			
10.0	39.81	15494.200	63.207	10.659	0.599	40.440			
10.0	63.10	18080.710	66.774	7.563	0.501	51.453			
10.0	100.0	20124.580	72.135	2.544	0.318	63.522			

Table 7. (continued) Components of Standard Uncertainty in the Loss Modulus G"								
Temperature	Frequency	Loss Modulus G"	<i>u</i> (G",Ф)	<i>u</i> (G", <i>h</i> )	<i>u</i> (G", <i>R</i> )	Tilt		
°C	rad/s	Pa	Pa	Pa	Pa	Pa		
10.0	0.1000	118.479	0.296	0.983	0.663	0.592		
10.0	0.1585	187.541	0.469	1.557	1.050	0.938		
10.0	0.2512	295.930	0.740	2.456	1.657	1.480		
10.0	0.3981	465.325	1.165	3.862	2.606	2.327		
10.0	0.6310	727.025	1.824	6.034	4.071	3.635		
10.0	1.000	1125.524	2.833	9.342	6.303	5.628		
10.0	1.585	1721.208	4.358	14.286	9.639	8.606		
10.0	2.512	2583.663	6.606	21.444	14.469	12.918		
10.0	3.981	3795.438	9.853	31.502	21.254	18.977		
10.0	6.310	5421.453	14.401	44.998	30.360	27.107		
10.0	10.00	7492.469	20.558	62.187	41.958	37.462		
10.0	15.85	9958.459	28.555	82.655	55.767	49.792		
10.0	25.12	12698.490	38.556	105.397	71.112	63.492		
10.0	39.81	15494.200	50.526	128.602	86.768	77.471		
10.0	63.10	18080.710	64.291	150.070	101.252	90.404		
10.0	100.0	20124.580	79.377	167.034	112.698	100.623		

Table 7. (co	Table 7. (continued) Components of Standard Uncertainty in the Loss Modulus G"								
Temperature	Frequency	Loss Modulus G"	Standard Uncertainty (Type A)	<i>u</i> (G", <i>T</i> )	u(G",Ω)	<i>u</i> (G", <b>M</b> )			
°C	40 d/a	Pa	Pa	Pa	Pa	D <sub>o</sub>			
- 'C	rad/s	Pa	Pa	Pa	Pa	Pa			
20.0	0.1000	96.363	0.581	0.192	$9 \times 10^{-3}$	0.212			
20.0	0.1585	152.274	0.880	0.309	0.015	0.324			
20.0	0.2512	240.832	1.389	0.490	0.024	0.502			
20.0	0.3981	379.259	2.266	0.767	0.038	0.779			
20.0	0.6310	594.428	3.505	1.183	0.058	1.211			
20.0	1.000	925.786	5.447	1.793	0.088	1.880			
20.0	1.585	1425.961	8.343	2.656	0.131	2.898			
20.0	2.512	2164.056	12.785	3.825	0.190	4.420			
20.0	3.981	3215.321	18.169	5.309	0.266	6.639			
20.0	6.310	4665.235	25.520	7.065	0.359	9.805			
20.0	10.00	6559.541	33.606	8.900	0.459	14.159			
20.0	15.85	8901.251	42.731	10.488	0.554	19.947			
20.0	25.12	11592.120	52.844	11.349	0.621	27.321			
20.0	39.81	14463.130	60.362	10.977	0.636	36.344			
20.0	63.10	17257.780	66.317	8.941	0.577	46.948			
20.0	100.0	19602.820	72.717	5.026	0.432	58.763			

Table 7. (continued) Components of Standard Uncertainty in the Loss Modulus G"								
Temperature	Frequency	Loss Modulus G"	<i>u</i> (G",Ф)	<i>u</i> (G", <i>h</i> )	<i>u</i> (G", <i>R</i> )	Tilt		
°C	rad/s	Pa	Pa	Pa	Pa	Pa		
20.0	0.1000	96.363	0.241	0.800	0.540	0.482		
20.0	0.1585	152.274	0.381	1.264	0.853	0.761		
20.0	0.2512	240.832	0.602	1.999	1.349	1.204		
20.0	0.3981	379.259	0.949	3.148	2.124	1.896		
20.0	0.6310	594.428	1.489	4.934	3.329	2.972		
20.0	1.000	925.786	2.325	7.684	5.184	4.629		
20.0	1.585	1425.961	3.598	11.835	7.985	7.130		
20.0	2.512	2164.056	5.501	17.962	12.119	10.820		
20.0	3.981	3215.321	8.274	26.687	18.006	16.077		
20.0	6.310	4665.235	12.231	38.721	26.125	23.326		
20.0	10.00	6559.541	17.674	54.444	36.733	32.798		
20.0	15.85	8901.251	24.909	73.880	49.847	44.506		
20.0	25.12	11592.120	34.126	96.215	64.916	57.961		
20.0	39.81	14463.130	45.406	120.044	80.994	72.316		
20.0	63.10	17257.780	58.661	143.240	96.644	86.289		
20.0	100.0	19602.820	73.429	162.703	109.776	98.014		

Table 7. (co	Table 7. (continued) Components of Standard Uncertainty in the Loss Modulus G"								
Temperature	Frequency	Loss Modulus	Standard Uncertainty	<i>u</i> (G", <i>T</i> )	u(G",Ω)	$u(G'',\mathbf{M})$			
		G"	(Type A)						
°C	rad/s	Pa	Pa	Pa	Pa	Pa			
30.0	0.1000	79.283	0.489	0.146	$8 \times 10^{-3}$	0.178			
30.0	0.1585	125.640	0.809	0.236	0.012	0.271			
30.0	0.2512	198.620	1.236	0.377	0.020	0.417			
30.0	0.3981	313.660	1.884	0.595	0.031	0.647			
30.0	0.6310	492.782	2.919	0.924	0.049	1.007			
30.0	1.000	770.069	4.618	1.413	0.074	1.565			
30.0	1.585	1192.843	7.000	2.116	0.112	2.421			
30.0	2.512	1820.693	11.685	3.085	0.164	3.707			
30.0	3.981	2737.736	16.068	4.367	0.234	5.619			
30.0	6.310	4022.379	22.691	5.940	0.321	8.373			
30.0	10.00	5745.912	31.016	7.691	0.422	12.232			
30.0	15.85	7935.413	41.150	9.372	0.525	17.446			
30.0	25.12	10537.330	49.719	10.579	0.610	24.219			
30.0	39.81	13418.020	59.814	10.835	0.653	32.672			
30.0	63.10	16330.680	68.034	9.660	0.631	42.772			
30.0	100.0	18938.980	72.159	6.745	0.524	54.295			

Table 7. (continued) Components of Standard Uncertainty in the Loss Modulus G"								
Temperature	Frequency	Loss Modulus G"	<i>u</i> (G",Ф)	<i>u</i> (G", <i>h</i> )	<i>u</i> (G", <i>R</i> )	Tilt		
°C	rad/s	Pa	Pa	Pa	Pa	Pa		
30.0	0.1000	79.283	0.198	0.658	0.444	0.396		
30.0	0.1585	125.640	0.314	1.043	0.704	0.628		
30.0	0.2512	198.620	0.497	1.649	1.112	0.993		
30.0	0.3981	313.660	0.785	2.603	1.756	1.568		
30.0	0.6310	492.782	1.234	4.090	2.760	2.464		
30.0	1.000	770.069	1.932	6.392	4.312	3.850		
30.0	1.585	1192.843	3.002	9.901	6.680	5.964		
30.0	2.512	1820.693	4.609	15.112	10.196	9.103		
30.0	3.981	2737.736	6.999	22.723	15.331	13.689		
30.0	6.310	4022.379	10.442	33.386	22.525	20.112		
30.0	10.00	5745.912	15.265	47.691	32.177	28.730		
30.0	15.85	7935.413	21.783	65.864	44.438	39.677		
30.0	25.12	10537.330	30.249	87.460	59.009	52.687		
30.0	39.81	13418.020	40.815	111.370	75.141	67.090		
30.0	63.10	16330.680	53.441	135.545	91.452	81.653		
30.0	100.0	18938.980	67.844	157.194	106.058	94.695		

Table 7. (co	Table 7. (continued) Components of Standard Uncertainty in the Loss Modulus G"								
Temperature	Frequency	Loss	Standard	<i>u</i> (G", <i>T</i> )	u(G",Ω)	$u(G'',\mathbf{M})$			
		Modulus	Uncertainty						
		G"	(Type A)						
°C	rad/s	Pa	Pa	Pa	Pa	Pa			
40.0	0.1000	66.056	0.402	0.113	$6 \times 10^{-3}$	0.152			
40.0	0.1585	104.538	0.669	0.183	0.010	0.229			
40.0	0.2512	165.513	1.032	0.293	0.016	0.351			
40.0	0.3981	261.608	1.653	0.465	0.026	0.543			
40.0	0.6310	411.694	2.543	0.727	0.041	0.844			
40.0	1.000	645.392	3.972	1.120	0.063	1.314			
40.0	1.585	1004.058	6.170	1.694	0.096	2.038			
40.0	2.512	1544.708	9.533	2.504	0.142	3.139			
40.0	3.981	2339.770	14.387	3.594	0.205	4.781			
40.0	6.310	3472.576	20.662	4.977	0.286	7.176			
40.0	10.00	5026.861	28.894	6.595	0.384	10.583			
40.0	15.85	7051.731	38.573	8.268	0.490	15.262			
40.0	25.12	9531.251	48.459	9.672	0.588	21.450			
40.0	39.81	12365.630	58.681	10.372	0.655	29.309			
40.0	63.10	15341.240	66.625	9.889	0.664	38.870			
40.0	100.0	18149.890	73.225	7.844	0.594	50.015			

Table 7. (continued) Components of Standard Uncertainty in the Loss Modulus G"								
Temperature	Frequency	Loss Modulus G"	<i>u</i> (G",Ф)	<i>u</i> (G", <i>h</i> )	<i>u</i> (G", <i>R</i> )	Tilt		
°C	rad/s	Pa	Pa	Pa	Pa	Pa		
40.0	0.1000	66.056	0.165	0.548	0.370	0.330		
40.0	0.1585	104.538	0.261	0.868	0.585	0.523		
40.0	0.2512	165.513	0.414	1.374	0.927	0.828		
40.0	0.3981	261.608	0.654	2.171	1.465	1.308		
40.0	0.6310	411.694	1.030	3.417	2.305	2.058		
40.0	1.000	645.392	1.617	5.357	3.614	3.227		
40.0	1.585	1004.058	2.523	8.334	5.623	5.020		
40.0	2.512	1544.708	3.899	12.821	8.650	7.724		
40.0	3.981	2339.770	5.952	19.420	13.103	11.699		
40.0	6.310	3472.576	8.946	28.822	19.446	17.363		
40.0	10.00	5026.861	13.204	41.723	28.150	25.134		
40.0	15.85	7051.731	19.053	58.529	39.490	35.259		
40.0	25.12	9531.251	26.788	79.109	53.375	47.656		
40.0	39.81	12365.630	36.611	102.635	69.248	61.828		
40.0	63.10	15341.240	48.563	127.332	85.911	76.706		
40.0	100.0	18149.890	62.493	150.644	101.639	90.749		

Table 7. (co	Table 7. (continued) Components of Standard Uncertainty in the Loss Modulus G"									
Temperature	Frequency	Loss	Standard	<i>u</i> (G", <i>T</i> )	u(G",Ω)	$u(G'',\mathbf{M})$				
		Modulus	Uncertainty							
		G"	(Type A)							
°C	rad/s	Pa	Pa	Pa	Pa	Pa				
50.0	0.1000	55.410	0.351	0.087	$5 \times 10^{-3}$	0.131				
50.0	0.1585	87.878	0.569	0.143	$9 \times 10^{-3}$	0.196				
50.0	0.2512	138.912	0.879	0.230	0.014	0.298				
50.0	0.3981	219.652	1.431	0.366	0.022	0.459				
50.0	0.6310	346.292	2.144	0.576	0.034	0.713				
50.0	1.000	544.440	3.390	0.894	0.054	1.111				
50.0	1.585	850.075	5.097	1.363	0.082	1.726				
50.0	2.512	1314.185	8.362	2.034	0.123	2.667				
50.0	3.981	2004.889	12.366	2.959	0.179	4.084				
50.0	6.310	3002.125	18.447	4.162	0.254	6.170				
50.0	10.00	4397.122	26.239	5.627	0.348	9.176				
50.0	15.85	6251.419	35.661	7.226	0.454	13.358				
50.0	25.12	8587.317	46.382	8.716	0.559	18.988				
50.0	39.81	11331.410	57.165	9.711	0.643	26.249				
50.0	63.10	14320.710	65.802	9.764	0.680	35.253				
50.0	100.0	17249.240	74.009	8.444	0.643	45.896				

Table 7. (continued) Components of Standard Uncertainty in the Loss Modulus G"								
Temperature	Frequency	Loss Modulus G"	<i>u</i> (G",Φ)	<i>u</i> (G", <i>h</i> )	<i>u</i> (G", <i>R</i> )	Tilt		
°C	rad/s	Pa	Pa	Pa	Pa	Pa		
50.0	0.1000	55.410	0.139	0.460	0.310	0.277		
50.0	0.1585	87.878	0.220	0.729	0.492	0.439		
50.0	0.2512	138.912	0.347	1.153	0.778	0.695		
50.0	0.3981	219.652	0.549	1.823	1.230	1.098		
50.0	0.6310	346.292	0.866	2.874	1.939	1.731		
50.0	1.000	544.440	1.363	4.519	3.049	2.722		
50.0	1.585	850.075	2.133	7.056	4.760	4.250		
50.0	2.512	1314.185	3.309	10.908	7.359	6.571		
50.0	3.981	2004.889	5.081	16.641	11.227	10.024		
50.0	6.310	3002.125	7.687	24.918	16.812	15.011		
50.0	10.00	4397.122	11.445	36.496	24.624	21.986		
50.0	15.85	6251.419	16.673	51.887	35.008	31.257		
50.0	25.12	8587.317	23.710	71.275	48.089	42.937		
50.0	39.81	11331.410	32.786	94.051	63.456	56.657		
50.0	63.10	14320.710	44.041	118.862	80.196	71.604		
50.0	100.0	17249.240	57.345	143.169	96.596	86.246		

#### 5. Conclusion

The measured viscosity and first normal stress difference data are given in Table 8, along with the combined standard uncertainties and the models fit to the data using equations (5) through (7).

The measured storage modulus G' and loss modulus G" are given in Table 9, along with the combined standard uncertainties and models fit to the data using equations (38) and (39).

An analysis of variance (ANOVA) was performed on the viscosity data to assess the bottle-tobottle variability and the effect of using different operators. The viscosity at the shear rate of 0.1 s<sup>-1</sup> was taken as a representative measurement for each experiment. Samples typically demonstrated viscosities that were consistently either above or below the mean over the whole range of shear rates that were tested, and 0.1 s<sup>-1</sup> lies in the middle of the range where the relative uncertainties are minimized, so this choice for a representative value is reasonable. At each temperature, two samples from each bottle were tested in random order. A different randomized order was used for each temperature. A one-way ANOVA indicated that bottle effects are significant; at 0 °C, the P-value is  $1.1 \times 10^{-4}$ ; at 25 °C, the P-value is  $9.3 \times 10^{-3}$ ; and at 50 °C, the P-value is  $6.8 \times 10^{-10}$ . The maximum relative deviation of a bottle mean from the overall mean was approximately 2 %. At each temperature, Operator 1 performed 11 experiments and Operator 2 performed 9 experiments. Each operator typically tested 2 or 3 samples on a given day, and a different random sequence at each temperature was used to choose the days each operator worked. A one-way ANOVA indicated that operator effects were not significant; at 0 °C, the P-value is 0.64; at 25 °C, the P-value is 0.93; and at 50 °C, the P-value is 0.32. The effect of testing sequence was also found to be insignificant, based on a straight-line fit of the representative viscosity as a function of the test sequence, with the standard uncertainty in the slopes indicating that the slopes are not significantly different from zero for all three temperatures.

As noted above in section 4.1.2, the relative Type A uncertainty in the viscosity increases significantly with increasing shear rate for the tests in steady shear at 0 °C and 25 °C. This increase is likely associated with instabilities at the edge of the cone and plate fixtures. This increase in the relative Type A uncertainty is reflected in a sharp increase in the relative combined standard uncertainty in the viscosity at 0 °C and 25 °C at the highest shear rate reported  $(6.310 \, \text{s}^{-1})$ . There was also some difficulty in modeling the viscosity data at the highest shear rates while incorporating both the expected time-temperature superposition behavior and the power-law behavior reported by the manufacturer [8]. Because of this sharp increase in the relative combined standard uncertainty and the difficulty in modeling the viscosity data, the viscosity and first normal stress difference data at  $6.310 \, \text{s}^{-1}$  have been included as reference values only.

Table 8. Viscosity ( $\eta$ ) and First Normal Stress Difference ( $N_1$ ) with Combined Standard Uncertainties and Models Fit to the Data									
Temperature	Shear Rate	Viscosit y η	Combined Standard Uncertaint y	Model Fit to Viscosity	$N_1$	Combined Standard Uncertainty	Model Fit to $N_1$		
°C	s <sup>-1</sup>	Pa·s	Pa·s	Pa·s	Pa	Pa	Pa		
0.0	0.001000	1472.40	15.49	1479.58					
0.0	0.001585	1472.93	15.43	1479.58					
0.0	0.002512	1473.68	14.91	1479.58					
0.0	0.003981	1476.55	14.93	1479.58					
0.0	0.006310	1474.53	14.94	1479.58					
0.0	0.01000	1476.26	14.87	1479.58					
0.0	0.01585	1476.39	14.81	1479.56					
0.0	0.02512	1475.86	14.81	1479.54					
0.0	0.03981	1475.19	14.79	1479.46					
0.0	0.06310	1475.14	14.77	1479.28					
0.0	0.1000	1474.36	14.77	1478.83	7.25	2.60	6.48		
0.0	0.1585	1470.27	14.68	1477.70	19.85	2.91	15.98		
0.0	0.2512	1465.33	14.60	1474.87	39.94	2.49	38.47		
0.0	0.3981	1455.25	14.48	1467.84	94.79	2.84	88.92		
0.0	0.6310	1435.87	14.00	1450.75	201.91	4.35	194.82		
0.0	1.000	1404.58	13.19	1410.99	423.75	6.95	406.83		
0.0	1.585	1356.37	11.93	1326.96	872.03	13.93	823.95		
0.0	2.512	1258.29	10.30	1178.30	1783.60	27.56	1643.22		
0.0	3.981	1033.87	7.96	973.99	3325.02	49.68	3254.84		
0.0	6.310	714.02*	6.45*	757.08	5546.10*	84.49*	6428.87		

<sup>\*</sup> These data are provided as reference values only (see section 5 for discussion).

Table 8. (continued) Viscosity ( $\eta$ ) and First Normal Stress Difference ( $N_1$ ) with Combined Standard Uncertainties and Models Fit to the Data									
Temperature	Shear Rate	Viscosit y η	Combined Standard Uncertaint	Model Fit to Viscosity	$N_1$	Combined Standard Uncertaint	Model Fit to $N_1$		
°C	s <sup>-1</sup>	Pa·s	y Pa·s	Pa⋅s	Pa	y Pa	Pa		
25.0	0.001000	841.58	9.55	843.87					
25.0	0.001585	842.57	9.16	843.87					
25.0	0.002512	844.64	8.78	843.87					
25.0	0.003981	843.45	8.78	843.87					
25.0	0.006310	844.89	8.53	843.87					
25.0	0.01000	844.80	8.50	843.87					
25.0	0.01585	844.82	8.48	843.86					
25.0	0.02512	844.83	8.46	843.86					
25.0	0.03981	844.59	8.46	843.85					
25.0	0.06310	844.22	8.45	843.82					
25.0	0.1000	844.14	8.43	843.75	2.59	0.91	1.99		
25.0	0.1585	843.17	8.44	843.56	5.40	0.96	4.98		
25.0	0.2512	841.67	8.41	843.10	11.88	1.03	12.34		
25.0	0.3981	839.55	8.39	841.93	29.23	1.13	30.03		
25.0	0.6310	833.78	8.31	839.04	68.02	1.70	70.58		
25.0	1.000	826.11	8.16	831.94	154.54	2.92	157.70		
25.0	1.585	810.03	7.76	815.08	337.51	5.71	334.48		
25.0	2.512	785.83	7.29	777.89	712.18	11.15	683.51		
25.0	3.981	727.75	6.68	707.03	1476.75	22.59	1368.90		
25.0	6.310	591.08*	6.86*	599.79	2755.87*	40.63*	2716.41		

<sup>\*</sup> These data are provided as reference values only (see section 5 for discussion).

Table 8. (continued) Viscosity ( $\eta$ ) and First Normal Stress Difference ( $N_1$ ) with Combined Standard Uncertainties and Models Fit to the Data									
Temperature	Shear Rate	Viscosit y η	Combined Standard Uncertaint y	Model Fit to Viscosit y	$N_1$	Combined Standard Uncertaint y	Model Fit to $N_1$		
°C	s <sup>-1</sup>	Pa·s	Pa·s	Pa·s	Pa	Pa	Pa		
50.0	0.001000	541.39	6.72	539.44					
50.0	0.001585	541.34	6.01	539.44					
50.0	0.002512	541.82	5.66	539.44					
50.0	0.003981	542.26	5.44	539.44					
50.0	0.006310	542.14	5.39	539.44					
50.0	0.01000	543.49	5.40	539.44					
50.0	0.01585	542.36	5.34	539.44					
50.0	0.02512	542.91	5.32	539.44					
50.0	0.03981	542.49	5.31	539.44					
50.0	0.06310	542.66	5.30	539.43					
50.0	0.1000	542.16	5.28	539.41					
50.0	0.1585	541.77	5.29	539.37					
50.0	0.2512	541.40	5.28	539.26					
50.0	0.3981	540.47	5.27	538.99	8.75	0.95	11.99		
50.0	0.6310	538.98	5.24	538.31	23.43	1.05	29.23		
50.0	1.000	535.59	5.19	536.61	58.93	1.46	68.99		
50.0	1.585	530.58	5.09	532.45	137.34	3.18	154.96		
50.0	2.512	519.97	4.88	522.50	308.37	5.18	330.16		
50.0	3.981	499.76	4.45	500.36	662.54	10.27	676.55		
50.0	6.310	422.09*	3.38*	457.40	1389.94*	25.84*	1356.80		

<sup>\*</sup> These data are provided as reference values only (see section 5 for discussion).

Table 9. Storage Modulus G' and Loss Modulus G' with the Combined Standard Uncertainties and Models Fit to the Data									
Temper- ature	Frequenc	Storage Modulus G'	Combined Standard Uncertaint y in G'	Model Fit to G'	Loss Modulus G"	Combined Standard Uncertaint y in G"	Model Fit to G"		
°C	rad/s	Pa	Pa	Pa	Pa	Pa	Pa		
0.0	0.1000	2.950	0.490	2.881	148.182	1.954	148.410		
0.0	0.1585	7.275	0.770	7.210	233.995	3.098	234.696		
0.0	0.2512	17.712	1.219	17.401	368.530	4.857	370.919		
0.0	0.3981	40.890	1.950	40.436	577.815	7.628	583.408		
0.0	0.6310	90.429	3.166	90.304	897.811	11.847	909.429		
0.0	1.000	193.601	5.209	193.468	1381.229	18.186	1399.122		
0.0	1.585	395.886	8.735	396.909	2092.364	27.354	2115.538		
0.0	2.512	775.449	14.839	778.335	3104.602	40.338	3130.774		
0.0	3.981	1448.818	24.859	1456.282	4491.832	58.320	4515.759		
0.0	6.310	2579.152	40.937	2595.045	6301.695	80.911	6321.885		
0.0	10.00	4359.395	65.297	4396.214	8526.568	108.350	8554.311		
0.0	15.85	6978.222	99.718	7067.401	11079.910	140.203	11141.189		
0.0	25.12	10589.670	145.360	10762.308	13797.660	173.685	13908.304		
0.0	39.81	15240.340	202.590	15496.220	16433.310	206.047	16572.838		
0.0	63.10	20890.950	270.563	21058.998	18743.830	236.976	18770.998		
0.0	100.0	27364.350	347.318	26962.176	20409.260	262.108	20124.797		

Table 9. (continued) Storage Modulus G' and Loss Modulus G' with the Combined Standard Uncertainties and Models Fit to the Data									
Temper- ature	Frequenc	Storage Modulus G'	Combined Standard Uncertaint y in G'	Model Fit to G'	Loss Modulus G"	Combined Standard Uncertaint y in G"	Model Fit to G"		
°C	rad/s	Pa	Pa	Pa	Pa	Pa	Pa		
10.0	0.1000	1.813	0.396	1.756	118.479	1.585	118.464		
10.0	0.1585	4.457	0.620	4.478	187.541	2.498	187.068		
10.0	0.2512	11.127	0.978	11.029	295.930	3.943	295.900		
10.0	0.3981	26.400	1.548	26.179	465.325	6.189	466.889		
10.0	0.6310	59.747	2.499	59.776	727.025	9.657	731.793		
10.0	1.000	130.639	4.062	131.072	1125.524	14.947	1134.638		
10.0	1.585	275.150	6.801	275.487	1721.208	22.793	1733.040		
10.0	2.512	553.661	11.425	554.016	2583.663	33.849	2596.742		
10.0	3.981	1061.283	19.212	1064.097	3795.438	49.579	3801.024		
10.0	6.310	1946.246	32.279	1948.477	5421.453	70.339	5412.683		
10.0	10.00	3388.485	52.512	3395.303	7492.469	96.282	7467.077		
10.0	15.85	5593.534	82.074	5620.094	9958.459	127.051	9938.026		
10.0	25.12	8752.303	123.294	8820.804	12698.490	160.865	12707.183		
10.0	39.81	12976.430	176.671	13103.341	15494.200	195.873	15544.683		
10.0	63.10	18287.190	241.330	18390.023	18080.710	228.566	18116.973		
10.0	100.0	24558.560	316.236	24340.110	20124.580	257.433	20033.027		

	Table 9. (continued) Storage Modulus G' and Loss Modulus G' with the Combined Standard Uncertainties and Models Fit to the Data									
Temper- ature	Frequenc y	Storage Modulus G'	Combined Standard Uncertaint y in G'	Model Fit to G'	Loss Modulus G"	Combined Standard Uncertaint y in G"	Model Fit to G"			
°C	rad/s	Pa	Pa	Pa	Pa	Pa	Pa			
20.0	0.1000	1.124	0.329	1.097	96.363	1.281	96.222			
20.0	0.1585	2.879	0.506	2.847	152.274	2.006	151.564			
20.0	0.2512	7.106	0.791	7.141	240.832	3.170	239.656			
20.0	0.3981	17.235	1.266	17.280	379.259	5.025	378.826			
20.0	0.6310	40.081	2.012	40.261	594.428	7.851	596.118			
20.0	1.000	89.693	3.241	90.166	925.786	12.214	929.939			
20.0	1.585	193.505	5.365	193.738	1425.961	18.780	1432.167			
20.0	2.512	397.996	9.052	398.677	2164.056	28.539	2168.390			
20.0	3.981	784.020	15.160	784.278	3215.321	42.021	3214.162			
20.0	6.310	1474.124	25.628	1472.243	4665.235	60.606	4644.871			
20.0	10.00	2636.350	42.140	2632.471	6559.541	84.326	6516.898			
20.0	15.85	4477.057	67.303	4475.428	8901.251	113.483	8840.051			
20.0	25.12	7208.341	103.568	7221.217	11592.120	147.185	11545.260			
20.0	39.81	10985.710	151.846	11038.257	14463.130	182.612	14456.767			
20.0	63.10	15897.750	213.255	15955.934	17257.780	217.777	17284.037			
20.0	100.0	21872.700	285.615	21771.542	19602.820	249.575	19647.696			

Table 9. (continued) Storage Modulus G' and Loss Modulus G' with the Combined Standard Uncertainties and Models Fit to the Data									
Temper- ature	Frequenc	Storage Modulus G'	Combined Standard Uncertaint y in G'	Model Fit to G'	Loss Modulus G"	Combined Standard Uncertaint y in G"	Model Fit to G"		
°C	rad/s	Pa	Pa	Pa	Pa	Pa	Pa		
30.0	0.1000	0.704	0.274	0.702	79.283	1.058	79.417		
30.0	0.1585	1.806	0.426	1.850	125.640	1.691	124.676		
30.0	0.2512	4.566	0.658	4.719	198.620	2.652	196.878		
30.0	0.3981	11.402	1.032	11.620	313.660	4.155	311.418		
30.0	0.6310	27.424	1.644	27.579	492.782	6.506	491.366		
30.0	1.000	62.974	2.644	62.967	770.069	10.187	770.141		
30.0	1.585	138.099	4.305	138.054	1192.843	15.703	1194.059		
30.0	2.512	289.962	7.202	290.132	1820.693	24.419	1823.727		
30.0	3.981	584.545	12.121	583.396	2737.736	36.009	2732.463		
30.0	6.310	1125.264	20.483	1120.394	4022.379	52.497	3999.431		
30.0	10.00	2065.874	34.245	2051.307	5745.912	74.425	5694.785		
30.0	15.85	3598.061	55.659	3574.014	7935.413	102.212	7855.554		
30.0	25.12	5946.615	87.105	5915.145	10537.330	134.138	10454.067		
30.0	39.81	9300.265	130.976	9282.550	13418.020	170.233	13365.526		
30.0	63.10	13793.150	187.747	13787.303	16330.680	206.908	16348.096		
30.0	100.0	19435.980	256.068	19347.070	18938.980	240.268	19050.859		

	Table 9. (continued) Storage Modulus G' and Loss Modulus G' with the Combined Standard Uncertainties and Models Fit to the Data								
Temper- ature	Frequenc	Storage Modulus G'	Combined Standard Uncertaint y in G'	Model Fit to G'	Loss Modulus G"	Combined Standard Uncertaint y in G"	Model Fit to G"		
°C	rad/s	Pa	Pa	Pa	Pa	Pa	Pa		
40.0	0.1000	0.451	0.233	0.459	66.056	0.878	66.517		
40.0	0.1585	1.239	0.356	1.228	104.538	1.404	104.006		
40.0	0.2512	3.126	0.553	3.179	165.513	2.208	163.889		
40.0	0.3981	7.772	0.861	7.955	261.608	3.499	259.174		
40.0	0.6310	18.987	1.364	19.202	411.694	5.477	409.605		
40.0	1.000	44.722	2.208	44.623	645.392	8.576	644.261		
40.0	1.585	100.166	3.542	99.663	1004.058	13.332	1004.307		
40.0	2.512	213.897	5.824	213.538	1544.708	20.520	1545.142		
40.0	3.981	439.351	9.754	438.118	2339.770	31.047	2336.408		
40.0	6.310	863.639	16.647	859.214	3472.576	45.757	3457.775		
40.0	10.00	1621.117	28.005	1607.750	5026.861	65.801	4987.675		
40.0	15.85	2891.034	46.226	2865.205	7051.731	91.546	6982.938		
40.0	25.12	4896.067	73.814	4854.348	9531.251	122.467	9449.428		
40.0	39.81	7845.696	113.010	7804.646	12365.630	157.806	12307.880		
40.0	63.10	11915.750	165.161	11886.125	15341.240	194.639	15365.959		
40.0	100.0	17188.690	230.921	17116.133	18149.890	230.413	18311.359		

	Table 9. (continued) Storage Modulus G' and Loss Modulus G' with the Combined Standard Uncertainties and Models Fit to the Data								
Temper- ature	Frequenc	Storage Modulus G'	Combined Standard Uncertaint y in G'	Model Fit to G'	Loss Modulus G"	Combined Standard Uncertaint y in G"	Model Fit to G"		
°C	rad/s	Pa	Pa	Pa	Pa	Pa	Pa		
50.0	0.1000	0.301	0.201	0.306	55.410	0.743	56.466		
50.0	0.1585	0.878	0.304	0.831	87.878	1.182	87.892		
50.0	0.2512	2.103	0.467	2.181	138.912	1.858	138.114		
50.0	0.3981	5.521	0.725	5.539	219.652	2.956	218.194		
50.0	0.6310	13.536	1.147	13.580	346.292	4.605	345.104		
50.0	1.000	32.173	1.815	32.076	544.440	7.247	544.186		
50.0	1.585	72.720	2.935	72.869	850.075	11.219	851.964		
50.0	2.512	159.061	4.789	158.934	1314.185	17.563	1318.742		
50.0	3.981	332.501	7.979	332.197	2004.889	26.602	2009.762		
50.0	6.310	665.395	13.608	664.205	3002.125	39.796	3003.065		
50.0	10.00	1274.141	22.954	1268.084	4397.122	57.941	4381.333		
50.0	15.85	2323.171	38.430	2307.524	6251.419	81.703	6215.185		
50.0	25.12	4025.386	62.367	3994.987	8587.317	111.294	8536.837		
50.0	39.81	6602.065	97.277	6568.469	11331.410	145.632	11306.238		
50.0	63.10	10259.591	144.945	10237.887	14320.710	182.468	14378.240		
50.0	100.0	15120.080	206.529	15099.672	17249.240	219.569	17484.194		

### 6. References

- 1. K. Walters, *Rheometry*, Chapman and Hall, London, 1975.
- 2. W.R. Schowalter, Mechanics of Non-Newtonian Fluids, Pergamon Press, Oxford, 1978.
- 3. R.I. Tanner, Engineering Rheology, Clarendon Press, Oxford, 1985.
- 4. R.B. Bird, R.C. Armstrong and O. Hassager, *Dynamics of Polymeric Liquids, Vol. 1, Fluid Mechanics*, 2nd Edition, John Wiley and Sons, New York, 1987.
- 5. R.B. Bird, C.F. Curtiss, R.C. Armstrong and O. Hassager, *Dynamics of Polymeric Liquids, Volume 2, Kinetic Theory*, 2nd Edition, John Wiley and Sons, New York, 1987.
- 6. C.W. Macosko, *Rheology Principles, Measurements and Applications*, Wiley-VCH, New York, 1994.
- 7. C.R. Schultheisz and S.D. Leigh, "Certification of the Rheological Behavior of SRM 2490, Polyisobutylene Dissolved in 2,6,10,14-Tetramethylpentadecane," NIST Special Publication 260-143, U.S. Department of Commerce, Technology Administration, National Institute of Standards and Technology, 2002.
- 8. *Gelest Silicone Fluids: Stable, Inert Media*, Gelest, Inc., Tullytown, PA, 1997. See also http://www.gelest.com/Library/SiFluids.pdf
- 9. Advanced Rheometric Expansion System ARES Instrument Manual, Rheometric Scientific, 1997.
- 10. J.V. Nicholas and D.R. White, *Traceable Temperatures*, John Wiley and Sons, Chichester, 1994.
- 11. B.N. Taylor, and C.E. Kuyatt, "Guidelines for Evaluating and Expressing the Uncertainty of NIST Measurement Results," NIST Technical Note 1297, 1994 Edition, U.S. Government Printing Office, Washington, D.C., 1994.
- 20. M.E. Mackay and G.K. Dick, "A comparison of the dimensions of a truncated cone measured with various techniques: The cone measurement project," *Journal of Rheology*, Volume 39, pp. 673-677, 1995.
- 21. R. Garritano, Rheometric Scientific, Incorporated, private communication.
- 22. J.M. Niemiec, J.-J. Pesce, G.B. McKenna, S. Skocypec and R.F. Garritano, "Anomalies in the Normal Force Measurement when using a Force Rebalance Transducer," *Journal of Rheology*, Volume 40, pp. 323-334, 1996.
- 23. Schultheisz, C.R. and McKenna, G.B., "Thermal Expansion and Its Effect on the Normal Force for a Modified Force Rebalance Transducer," *Proceedings of SPE ANTEC*, Volume 1, Processing, pp. 1142-1145, May 3-6, 1999.
- 24. H. Markovitz, L.J. Elyash, F.J. Padden, Jr. and T.W. DeWitt, "A Cone-and-Plate Viscometer," *Journal of Colloid Science*, Volume 10, p. 165-173, 1955.
- 25. W.H. Press, S.A. Teukolsky, W.T. Vetterling and B.P. Flannery, *Numerical Recipes*, Second Edition, Cambridge University Press, Cambridge, 1992.
- 26. G.V. Gordon and M.T. Shaw, *Computer Programs for Rheologists*, Hanser Publishers, Munich, 1994.
- 27. B.D. Marsh and J.R.A. Pearson, "The Measurement of Normal-Stress Differences Using a Cone-and-Plate Total Thrust Apparatus," *Rheologica Acta*, Volume 7, pp. 326-331, 1968.
- 28. G. Winther, D.M. Parsons and J.L. Schrag, "A High-Speed, High-Precision Data Acquisition and Processing System for Experiments Producing Steady State Periodic Signals," *Journal of Polymer Science: Part B: Polymer Physics*, Volume 32, pp. 659-670, 1994.
- 29. RMS-800/RDS-II Instrument Manual, Rheometric Scientific, 1990.



# Certificate of Analysis

## Standard Reference Material® 2491

## Non-Newtonian Polymer Melt for Rheology

## Polydimethylsiloxane

This Standard Reference Material (SRM) is intended primarily for use in calibration and performance evaluation of instruments used to determine the viscosity and first normal stress difference in steady shear, or to determine the dynamic mechanical storage and loss moduli and shift factors through time-temperature superposition. SRM 2491 consists of polydimethylsiloxane. The supplier identifies the polydimethylsiloxane as having a number average molecular mass of 308,000 g/mol. One unit of SRM 2491 consists of 100 mL of the fluid packaged in an amber glass bottle.

Certified Values and Uncertainties: The certified values of the viscosity and first normal stress difference as functions of shear rate are given in Tables 4a, 4b, and 4c at temperatures of 0 °C, 25 °C, and 50 °C, respectively. Tables 4a through 4c also list the expanded combined uncertainties in the certified values of the viscosity and first normal stress difference. Tables 5a, 5b, 5c, 5d, 5e, and 5f list the certified values of the storage modulus G' and loss modulus G' as functions of frequency at 0 °C, 10 °C, 20 °C, 30 °C, 40 °C, and 50 °C, respectively. Tables 5a through 5f also list the expanded combined uncertainties in the certified values of the storage modulus G' and loss modulus G''. The uncertainties in Tables 4a through 4c and 5a through 5f were calculated as  $U = ku_c$ , where k = 2 is the coverage factor for a 95 % level of confidence and  $u_c$  is the combined standard uncertainty calculated according to the ISO Guide [1].

**Expiration of Certification:** The certification of SRM 2491 is valid until **31 December 2012**, within the measurement uncertainties specified, provided that the SRM is handled in accordance with the storage instructions given in this certificate. This certification is nullified if the SRM is modified or contaminated.

**Maintenance of SRM Certification:** NIST will monitor this SRM over the period of its certification. If substantive technical changes occur that affect the certification before expiration of this certificate, NIST will notify the purchaser. Return of the attached registration card will facilitate notification.

Technical coordination leading to the certification of this SRM was provided by B.M. Fanconi of the NIST Polymers Division.

The certification of this SRM was performed by C.R. Schultheisz and K.M. Flynn of the NIST Polymers Division.

The support aspects in the preparation, certification, and issuance of this SRM were coordinated through the NIST Standard Reference Materials Group by J.W.L. Thomas and B.S. MacDonald.

Eric J. Amis, Chief Polymers Division

Gaithersburg, MD 20899 Certificate Issue Date: 31 December 2002 John Rumble, Jr., Chief Measurement Services Division

SRM 2491 Page 1 of 14

Technical assistance and advice were provided by G.F. Strouse and D.C. Vaughn of the NIST Process Measurements Division and G.B. McKenna of the Texas Tech University.

Statistical analysis and measurement advice were provided by S.D. Leigh of the NIST Statistical Engineering Division.

**Source of Material:** The polydimethylsiloxane was supplied by Gelest, Inc., Tullytown, PA.<sup>1</sup> The material was also homogenized and packaged by Gelest, Inc., Tullytown, PA.<sup>1</sup>

**Storage and Handling:** The SRM should be stored in the original bottle with the lid tightly closed under normal laboratory conditions. Before taking a sample, the bottle should be turned end-over-end at a rate of approximately 1 revolution per 10 minutes for 30 minutes. This procedure is intended to ensure that the material in each bottle is homogeneous, in case there is any settling caused by gravity.

**Homogeneity and Characterization:** The homogeneity of SRM 2491 was assessed using the zero-shear-rate viscosity measured at 25 °C using samples from 10 bottles randomly chosen from the 273 bottles available. The characterization of this polymer melt is described in reference 2.

Measurement Technique: All rheological testing was carried out using a Rheometric Scientific, Inc., ARES controlled-strain rheometer.<sup>1</sup> Transducer calibration was accomplished, in accordance with the manufacturer's instructions, by hanging a known mass from a fixture mounted to the transducer to apply a known torque or normal force. Phase angle calibration was accomplished, also in accordance with the manufacturer's instructions, by applying an oscillatory strain to an elastic steel test coupon. Temperature calibration in the rheometer was accomplished through comparison with a NIST-calibrated thermistor. The viscosity and first normal stress difference were measured in steady shear using 50 mm diameter, 0.04 rad cone-and-plate fixtures. The storage modulus and loss modulus were measured in 50 mm diameter parallel-plate fixtures with an applied strain magnitude of 2 % at a nominal gap of 1 mm.

**Models for the Data:** The steady shear data (viscosity and first normal stress difference) and the oscillatory data (storage modulus and loss modulus) were fitted to empirical functions to describe master curves and calculate shift factors for time-temperature superposition. These models can be used to estimate the rheological behavior of the material in the temperature range 0 °C to 50 °C.

**Models for the Steady Shear Data:** The viscosity  $\eta(\dot{\gamma}, T)$  as a function of the shear rate  $\dot{\gamma}$ , and the temperature T was fitted to a Carreau model [3,4,5] of the form

$$\eta(\dot{\gamma}, T) = \left(\frac{T\rho}{T_R \rho_R}\right) \eta_R a(T) \left[1 + (\xi_0 a(T)\dot{\gamma})^2\right]^{(n-1)/2}$$
(1)

where  $\rho$  is the density at temperature T,  $\eta_R$  is the zero-shear-rate viscosity at the reference temperature  $T_R = 25$  °C,  $\rho_R$  is the density at the reference temperature  $T_R$ ,  $\xi_0$  is a parameter that governs the transition from the Newtonian regime at low shear rates to the power law regime at high shear rates,  $\alpha(T)$  is the temperature shift factor, and n is the power at which the shear stress increases with shear rate. Based on data from the manufacturer [6], n has been set equal to 0.3. The density was approximated as a linear function of temperature, with  $\rho(T) = \rho_R (1 - \alpha(T - T_R))$ , where  $\alpha = 9.2 \times 10^{-4} \text{ cm}^3/(\text{cm}^3 \text{ K})$  [6] is the volumetric coefficient of thermal expansion. The shift factor  $\alpha(T)$  was fitted with a function of the WLF type [3],

$$a(T) = \exp\left(\frac{-C_1(T - T_R)}{C_2 + T - T_R}\right)$$
 (2)

SRM 2491 Page 2 of 14

<sup>&</sup>lt;sup>1</sup>Certain commercial equipment, instruments, or materials are identified in this certificate in order to adequately specify the experimental procedure. Such identification does not imply recommendation or endorsement by the National Institute of Standards and Technology, nor does it imply that the materials or equipment identified are necessarily the best available for the purpose.

The parameters  $\eta_R$ ,  $\xi_0$ , n,  $C_1$ , and  $C_2$  estimated from the fit to the viscosity data are given in Table 1.

Parameter	Value	Standard Uncertainty
$\eta_{\scriptscriptstyle R}$	843.9 Pa·s	3.8 Pa·s
$\xi_0$	0.2037 s	0.0040 s
n	0.3 [6]	
$C_1$	5.20	0.48
$C_2$	232 °C	21 °C

Table 1. Parameters for  $\eta(\dot{\gamma}, T)$  and a(T)

The first normal stress difference  $N_1(\dot{\gamma}, T)$  was fitted to a similar empirical model using the same temperature shift factor a(T) calculated from the viscosity data:

$$N_{1}(\dot{\gamma},T) = \left(\frac{T\rho}{T_{R}\rho_{R}}\right)\psi_{R}(a(T)\dot{\gamma})^{2}\left[1 + (\xi_{1}a(T)\dot{\gamma})^{2}\right]^{(m-1)/2}$$
(3)

where  $\rho$  is the density at temperature T;  $\psi_R$  is the zero-shear-rate first normal stress coefficient at the reference temperature  $T_R$  and  $\xi_1$  and  $\xi_2$  and  $\xi_3$  and  $\xi_4$  are parameters estimated from the fit to the data. The density was approximated as a linear function of temperature, with  $\rho(T) = \rho_R (1 - \alpha(T - T_R))$ , where  $\alpha = 9.2 \times 10^{-4}$  cm<sup>3</sup>/(cm<sup>3</sup> K) [6]. Values for the parameters describing  $N_1(\dot{\gamma}, T)$  are given in Table 2.

 Parameter
 Value
 Standard Uncertainty

  $\psi_R$   $200.2 \text{ Pa·s}^2$   $9.6 \text{ Pa·s}^2$ 
 $\xi_1$  1.22 s 0.33 s 

 m 0.474 0.069

Table 2. Parameters for  $N_1(\dot{\gamma}, T)$ 

**Models for the Oscillatory Data:** The storage modulus  $G'(\Omega,T)$  and loss modulus  $G''(\Omega,T)$  as functions of the frequency of oscillation  $\Omega$  and temperature T were modeled using polynomial functions [4]. The data were fitted to functions of the form

$$\ln\left(\frac{G'(\Omega, T)}{1 \text{ Pa}}\right) = \ln\left(\frac{T\rho}{T_R \rho_R}\right) + \sum_{k=0}^{3} p_k \left(\ln\left(\frac{a(T)\Omega}{1 \text{ rad/s}}\right)\right)^k$$

$$\ln\left(\frac{G''(\Omega, T)}{1 \text{ Pa}}\right) = \ln\left(\frac{T\rho}{T_R \rho_R}\right) + \sum_{k=0}^{3} q_k \left(\ln\left(\frac{a(T)\Omega}{1 \text{ rad/s}}\right)\right)^k$$
(4)

SRM 2491 Page 3 of 14

where  $\rho$  is the density at temperature T, and  $\rho_R$  is the density at the reference temperature  $T_R$  = 25 °C. The density was again approximated as a linear function of temperature, with  $\rho(T) = \rho_R (1 - \alpha (T - T_R))$ , where  $\alpha = 9.2 \times 10^{-4} \, \mathrm{cm}^3/(\mathrm{cm}^3 \, \mathrm{K})$ . The shift factor a(T) again was fitted with a function of the WLF type [3],

$$a(T) = \exp\left(\frac{-C_1(T - T_R)}{C_2 + T - T_R}\right)$$
 (5)

The parameters estimated from the oscillatory data are given in Table 3.

Table 3. Parameters for  $G'(\Omega, T)$ ,  $G''(\Omega, T)$  and a(T)

Parameter	Value	Standard Uncertainty
$p_0$	4.2508	$2.0 \times 10^{-3}$
$p_1$	1.72838	$8.7 \times 10^{-4}$
$p_2$	$-9.658 \times 10^{-2}$	$4.6 \times 10^{-4}$
$p_3$	$-3.09 \times 10^{-3}$	$1.1 \times 10^{-4}$
$q_0$	6.6701	$1.8 \times 10^{-3}$
$q_1$	0.95974	$8.6 \times 10^{-4}$
$q_2$	$-2.790 \times 10^{-2}$	$4.5 \times 10^{-4}$
$q_3$	$-7.13 \times 10^{-3}$	$1.1 \times 10^{-4}$
$C_1$	6.64	0.21
$C_2$	299.4 °C	9.2 °C

SRM 2491 Page 4 of 14

Table 4a. Certified Values of Viscosity and First Normal Stress Difference with Expanded Combined Uncertainties at 0  $^{\circ}$ C

Temperature	Shear Rate	Certified Value of the Viscosity, η	Uncertainty in the Viscosity	Certified Value of the First Normal Stress Difference, N <sub>1</sub>	Uncertainty in $N_1$
°C	$\mathrm{s}^{-1}$	Pa·s	Pa⋅s	Pa	Pa
0.0	0.001000	1472	31		
0.0	0.001585	1473	31		
0.0	0.002512	1474	30		
0.0	0.003981	1477	30		
0.0	0.006310	1475	30		
0.0	0.01000	1476	30		
0.0	0.01585	1476	30		
0.0	0.02512	1476	30		
0.0	0.03981	1475	30		
0.0	0.06310	1475	30		
0.0	0.1000	1474	30	7.26	5.20
0.0	0.1585	1470	29	19.8	5.8
0.0	0.2512	1465	29	39.9	5.0
0.0	0.3981	1455	29	94.8	5.7
0.0	0.6310	1436	28	201.9	8.7
0.0	1.000	1405	26	423.7	13.9
0.0	1.585	1356	24	872.0	27.9
0.0	2.512	1258	21	1784	55
0.0	3.981	1034	16	3325	99
0.0	6.310	714.0*	12.9*	5546*	169*

<sup>\*</sup> These data are provided as reference values only [2].

SRM 2491 Page 5 of 14

Table 4b. Certified Values of Viscosity and First Normal Stress Difference with Expanded Combined Uncertainties at 25 °C

Temperature	Shear Rate	Certified Value of the Viscosity, η	Uncertainty in the Viscosity	Certified Value of the First Normal Stress Difference, N <sub>1</sub>	Uncertainty in $N_1$
°C	$s^{-1}$	Pa∙s	Pa∙s	Pa	Pa
25.0	0.001000	841.6	19.1		
25.0	0.001585	842.6	18.3		
25.0	0.002512	844.6	17.6		
25.0	0.003981	843.5	17.6		
25.0	0.006310	844.9	17.1		
25.0	0.01000	844.8	17.0		
25.0	0.01585	844.8	17.0		
25.0	0.02512	844.8	16.9		
25.0	0.03981	844.6	16.9		
25.0	0.06310	844.2	16.9		
25.0	0.1000	844.1	16.9	2.59	1.83
25.0	0.1585	843.2	16.9	5.40	1.91
25.0	0.2512	841.7	16.8	11.9	2.1
25.0	0.3981	839.5	16.8	29.2	2.3
25.0	0.6310	833.8	16.6	68.0	3.4
25.0	1.000	826.1	16.3	154.5	5.8
25.0	1.585	810.0	15.5	337.5	11.4
25.0	2.512	785.8	14.6	712.2	22.3
25.0	3.981	727.7	13.4	1477	45
25.0	6.310	591.1*	13.7*	2756*	81*

<sup>\*</sup> These data are provided as reference values only [2].

SRM 2491 Page 6 of 14

Table 4c. Certified Values of Viscosity and First Normal Stress Difference with Expanded Combined Uncertainties at 50  $^{\circ}\mathrm{C}$ 

Temperature	Shear Rate	Certified Value of the Viscosity, η	Uncertainty in the Viscosity	Certified Value of the First Normal Stress Difference, N <sub>1</sub>	Uncertainty in $N_1$
°C	$\mathrm{s}^{-1}$	Pa·s	Pa⋅s	Pa	Pa
50.0	0.001000	541.4	13.4		
50.0	0.001585	541.3	12.0		
50.0	0.002512	541.8	11.3		
50.0	0.003981	542.3	10.9		
50.0	0.006310	542.1	10.8		
50.0	0.01000	543.5	10.8		
50.0	0.01585	542.4	10.7		
50.0	0.02512	542.9	10.6		
50.0	0.03981	542.5	10.6		
50.0	0.06310	542.7	10.6		
50.0	0.1000	542.2	10.6		
50.0	0.1585	541.8	10.6		
50.0	0.2512	541.4	10.6		
50.0	0.3981	540.5	10.5	8.8	1.9
50.0	0.6310	539.0	10.5	23.4	2.1
50.0	1.000	535.6	10.4	58.9	2.9
50.0	1.585	530.6	10.2	137.3	6.4
50.0	2.512	520.0	9.8	308.4	10.4
50.0	3.981	499.8	8.9	662.5	20.5
50.0	6.310	422.1*	6.8*	1390*	52*

<sup>\*</sup> These data are provided as reference values only [2].

SRM 2491 Page 7 of 14

Table 5a. Certified Values of the Storage Modulus G' and the Loss Modulus G' with Expanded Combined Uncertainties at 0  $^{\circ}\text{C}$ 

Temperature	Frequency of Oscillation	Certified Value of the Storage Modulus G'	Uncertainty in G'	Certified Value of the Loss Modulus G"	Uncertainty in G"
°C	rad/s	Pa	Pa	Pa	Pa
0.0	0.1000	2.95	0.98	148.2	3.9
0.0	0.1585	7.27	1.54	234.0	6.2
0.0	0.2512	17.7	2.4	368.5	9.7
0.0	0.3981	40.9	3.9	577.8	15.3
0.0	0.6310	90.4	6.3	897.8	23.7
0.0	1.000	193.6	10.4	1381	36
0.0	1.585	395.9	17.5	2092	55
0.0	2.512	775.4	29.7	3105	81
0.0	3.981	1449	50	4492	117
0.0	6.310	2579	82	6302	162
0.0	10.00	4359	131	8527	217
0.0	15.85	6978	199	11080	280
0.0	25.12	10590	291	13798	347
0.0	39.81	15240	405	16433	412
0.0	63.10	20891	541	18744	474
0.0	100.0	27364	695	20409	524

SRM 2491 Page 8 of 14

Table 5b. Certified Values of the Storage Modulus G' and the Loss Modulus G' with Expanded Combined Uncertainties at 10  $^{\circ}\mathrm{C}$ 

Temperature	Frequency of Oscillation	Certified Value of the Storage Modulus G'	Uncertainty in G'	Certified Value of the Loss Modulus G"	Uncertainty in G"
°C	rad/s	Pa	Pa	Pa	Pa
10.0	0.1000	1.81	0.79	118.5	3.2
10.0	0.1585	4.46	1.24	187.5	5.0
10.0	0.2512	11.1	2.0	295.9	7.9
10.0	0.3981	26.4	3.1	465.3	12.4
10.0	0.6310	59.8	5.0	727.0	19.3
10.0	1.000	130.6	8.1	1126	30
10.0	1.585	275.2	13.6	1721	46
10.0	2.512	553.7	22.9	2584	68
10.0	3.981	1061	38	3795	99
10.0	6.310	1946	65	5421	141
10.0	10.00	3388	105	7492	193
10.0	15.85	5594	164	9958	254
10.0	25.12	8752	247	12698	322
10.0	39.81	12976	353	15494	392
10.0	63.10	18287	483	18081	457
10.0	100.0	24559	632	20125	515

SRM 2491 Page 9 of 14

Table 5c. Certified Values of the Storage Modulus G' and the Loss Modulus G' with Expanded Combined Uncertainties at 20  $^{\circ}\mathrm{C}$ 

Temperature	Frequency of Oscillation	Certified Value of the Storage Modulus G'	Uncertainty in G'	Certified Value of the Loss Modulus G"	Uncertainty in G"
°C	rad/s	Pa	Pa	Pa	Pa
20.0	0.1000	1.12	0.66	96.4	2.6
20.0	0.1585	2.88	1.01	152.3	4.0
20.0	0.2512	7.11	1.58	240.8	6.3
20.0	0.3981	17.2	2.5	379.3	10.0
20.0	0.6310	40.1	4.0	594.4	15.7
20.0	1.000	89.7	6.5	925.8	24.4
20.0	1.585	193.5	10.7	1426	38
20.0	2.512	398.0	18.1	2164	57
20.0	3.981	784.0	30.3	3215	84
20.0	6.310	1474	51	4665	121
20.0	10.00	2636	84	6560	169
20.0	15.85	4477	135	8901	227
20.0	25.12	7208	207	11592	294
20.0	39.81	10986	304	14463	365
20.0	63.10	15898	427	17258	436
20.0	100.0	21873	571	19603	499

SRM 2491 Page 10 of 14

Table 5d. Certified Values of the Storage Modulus G' and the Loss Modulus G' with Expanded Combined Uncertainties at 30  $^{\circ}\mathrm{C}$ 

Temperature	Frequency of Oscillation	Certified Value of the Storage Modulus G'	Uncertainty in G'	Certified Value of the Loss Modulus G"	Uncertainty in G"
°C	rad/s	Pa	Pa	Pa	Pa
30.0	0.1000	0.704	0.548	79.3	2.1
30.0	0.1585	1.81	0.85	125.6	3.4
30.0	0.2512	4.57	1.32	198.6	5.3
30.0	0.3981	11.4	2.1	313.7	8.3
30.0	0.6310	27.4	3.3	492.8	13.0
30.0	1.000	63.0	5.3	770.1	20.4
30.0	1.585	138.1	8.6	1193	31
30.0	2.512	290.0	14.4	1821	49
30.0	3.981	584.5	24.2	2738	72
30.0	6.310	1125	41	4022	105
30.0	10.00	2066	68	5746	149
30.0	15.85	3598	111	7935	204
30.0	25.12	5947	174	10537	268
30.0	39.81	9300	262	13418	340
30.0	63.10	13793	375	16331	414
30.0	100.0	19436	512	18939	481

SRM 2491 Page 11 of 14

Table 5e. Certified Values of the Storage Modulus G' and the Loss Modulus G' with Expanded Combined Uncertainties at 40  $^{\circ}\mathrm{C}$ 

Temperature	Frequency of Oscillation	Certified Value of the Storage Modulus G'	Uncertainty in G'	Certified Value of the Loss Modulus G"	Uncertainty in G"
°C	rad/s	Pa	Pa	Pa	Pa
40.0	0.1000	0.451	0.466	66.1	1.8
40.0	0.1585	1.24	0.71	104.5	2.8
40.0	0.2512	3.13	1.11	165.5	4.4
40.0	0.3981	7.77	1.72	261.6	7.0
40.0	0.6310	19.0	2.7	411.7	11.0
40.0	1.000	44.7	4.4	645.4	17.2
40.0	1.585	100.2	7.1	1004	27
40.0	2.512	213.9	11.7	1544.71	41
40.0	3.981	439.4	19.5	2339.77	62
40.0	6.310	863.6	33.3	3472.58	92
40.0	10.00	1621	56	5026.86	132
40.0	15.85	2891	92	7051.73	183
40.0	25.12	4896	148	9531.25	245
40.0	39.81	7846	226	12365.63	316
40.0	63.10	11916	330	15341.24	389
40.0	100.0	17189	462	18149.89	461

SRM 2491 Page 12 of 14

Table 5f. Certified Values of the Storage Modulus G' and the Loss Modulus G' with Expanded Combined Uncertainties at 50  $^{\circ}\mathrm{C}$ 

Temperature	Frequency of Oscillation	Certified Value of the Storage Modulus G'	Uncertainty in G'	Certified Value of the Loss Modulus G"	Uncertainty in G"
°C	rad/s	Pa	Pa	Pa	Pa
50.0	0.1000	0.301	0.401	55.4	1.5
50.0	0.1585	0.878	0.607	87.9	2.4
50.0	0.2512	2.10	0.93	138.9	3.7
50.0	0.3981	5.52	1.45	219.7	5.9
50.0	0.6310	13.5	2.3	346.3	9.2
50.0	1.000	32.2	3.6	544.4	14.5
50.0	1.585	72.7	5.9	850.1	22.4
50.0	2.512	159.1	9.6	1314	35
50.0	3.981	332.5	16.0	2005	53
50.0	6.310	665.4	27.2	3002	80
50.0	10.00	1274	46	4397	116
50.0	15.85	2323	77	6251	163
50.0	25.12	4025	125	8587	223
50.0	39.81	6602	195	11331	291
50.0	63.10	10260	290	14321	365
50.0	100.0	15120	413	17249	439

SRM 2491 Page 13 of 14

#### REFERENCES

- [1] Guide to the Expression of Uncertainty in Measurement; ISBN 92-67-10188-9, 1st Ed. ISO, Geneva, Switzerland (1993); see also Taylor, B.N.; Kuyatt, C.E.; Guidelines for Evaluating and Expressing the Uncertainty of NIST Measurement Results; NIST Technical Note 1297, U.S. Government Printing Office, Washington, DC (1994); available at <a href="http://physics.nist.gov/Pubs/">http://physics.nist.gov/Pubs/</a>.
- [2] Schultheisz, C.R.; Flynn, K.M.; Leigh, S.D.; *Certification of the Rheological Behavior of SRM 2491, Polydimethylsiloxane*; NIST Special Publication 260-147, U.S. Department of Commerce, Technology Administration, National Institute of Standards and Technology (2001).
- [3] Macosko, C.W.; Rheology Principles, Measurements and Applications; Wiley-VCH, New York (1994).
- [4] Gordon, G.V.; Shaw, M.T.; Computer Programs for Rheologists; Hanser Publishers, Munich (1994).
- [5] Bird, R.B.; Armstrong, R.C.; Hassager, O.; *Dynamics of Polymeric Liquids, Vol. 1, Fluid Mechanics*, 2nd Edition, John Wiley and Sons, New York (1987).
- [6] Gelest Silicone Fluids: Stable, Inert Media, Gelest, Inc., Tullytown, PA (1997); available at <a href="http://www.gelest.com/Library/SiFluids.pdf">http://www.gelest.com/Library/SiFluids.pdf</a>.

Users of this SRM should ensure that the certificate in their possession is current. This can be accomplished by contacting the SRM Group at: telephone (301) 975-6776; fax (301) 926-4751; e-mail srminfo@nist.gov; or via the Internet <a href="http://www.nist.gov/srm">http://www.nist.gov/srm</a>.

SRM 2491 Page 14 of 14